METHANE FLUXES FROM A NORTHERN PEATLAND: MECHANISMS CONTROLLING DIURNAL AND SEASONAL VARIATION AND THE MAGNITUDE OF AEROBIC METHANOGENESIS

KEVIN D. LONG

Bachelor of Science, University of Lethbridge, 2006

A Thesis Submitted to the School of Graduate Studies of the University of Lethbridge in Partial Fulfilment of the Requirements for the Degree

MASTER OF SCIENCE

Department of Biological Sciences
University of Lethbridge
LETHBRIDGE, ALBERTA, CANADA

Abstract

Continuous eddy covariance measurements were conducted for a 125 day period, throughout the 2007 growing season, in a northern Alberta peatland. Significant diurnal and seasonal variation in methane fluxes were observed. Diurnal variation in methane flux was suggested to be due to variation in soil temperature and methane convective flow through vegetation to the atmosphere. Seasonal variation in methane flux was associated with a variety of factors, most notably seasonal variation in the capacity for methane emission at 10 ºC (R_{10}). The R_{10} values varied as a function of soil temperature and were an important control of seasonal variation in methane flux. Also, a greenhouse gas budget was calculated comparing net methane emission and net CO_2 sequestration. This analysis indicated that the peatland was acting as a net sink of radiative forcing agents for the 2007 growing season.

Acknowledgements

I would like to thank my thesis supervisor, Dr. Lawrence B. Flanagan, for the teaching, guidance and research funding he provided throughout my study. Dr. Flanagan served as a mentor, teacher and role model, serving as an example of what is necessary in order to be successful in research and in life. Funding for this research was provided by grants to Dr. Flanagan from the Natural Sciences and Engineering Research Council of Canada (NSERC) and the Canadian Foundation for Climate and Atmospheric Sciences (CFCAS).

I am grateful for the assistance provided by my thesis committee: Dr. John Bain and Dr. Mathew Letts. For the course of my study committee meetings were an invaluable tool providing me with direction needed to be successful within a graduate program.

I am appreciative of funding provided by the Canadian Carbon Program (CCP) and the Fluxnet Canada Research Network (FCRN). This funding accounted for 50 % of travel and registration expenses when attending conferences and courses.

Lastly, I am thankful to my friends and family who have been both supportive and tolerant throughout my study. Specifically, my father, for helping me throughout my entire academic career, my brothers, nieces and nephews, for making me smile and my companion Sara, for always giving me a reason to be thankful for every day of life.

Contents

Tables

Figures

Symbols

NEE	Net ecosystem exchange
PAR	Photosynthetically active radiation
PPFD	Photosynthetic photon flux density
GPP	Gross primary productivity
WT	Water table depth
Ts	Soil temperature (average of a 20 cm hollow and 50 cm hummock)
S	Substrate availability (preceding 10 day average)
UVA	Ultraviolet A light (315 - 400 nm)
UVB	Ultraviolet B light (280 - 314 nm)
u^*	Measure of friction velocity
R_{10}	Capacity of net methane emission at 10 ºC

Introduction

Peatlands play an important role in the global carbon cycle, by sequestering large quantities of CO_2 and emitting the second most important greenhouse trace gas (after CO_2), methane. Methane emitted from peatlands contributes significantly to greenhouse warming, since each methane molecule has a warming potential nearly thirty times greater than a CO_2 molecule (IPCC, 2001). Numerous previous research efforts have been conducted in order to quantify methane flux from peatlands, and also to identify the environmental factors that influence methane flux (Heyer and Berger, 2000; Hirota et al., 2004; Joabsson and Christensen, 2001; Moore and Roulet, 1993; Morrissey et al., 1993; Seiler et al., 1984; Verma et al., 1992). To date, the vast majority of studies have used closed chamber systems in order to measure methane flux. As an alternative to chamber measurements, some studies have measured methane flux through the use of an eddy-covariance sampling system (Billesbach et al., 1988; Fan et al., 1992; Sachs et al., 2008; Verma et al., 1992). The eddy covariance measurement technique measures integrated methane flux over a large area, is non-intrusive and can provide continuous flux measurements. The measurement of methane flux via eddy covariance has provided insights into possible new controls that were not observed with previous chamber measurements. These new insights illustrate the need for further investigation to validate newly proposed controls of net methane emission. By conducting further eddy covariance methane flux studies, a better understanding of the factors controlling methane flux can be gained.

The majority of field campaigns that have measured methane flux have been conducted in wetlands. This is because several previous studies indicated that significant methane production only occurs in water logged anaerobic environments. However, some recent studies have suggested that methane can be produced by plants under aerobic conditions (Keppler et al., 2006). Only a few studies have provided independent verification of aerobic methane emission by plants (Sanhueza and Donoso, 2006; Vigano et al., 2008), but some current research has identified possible precursors of methane within the normal biochemical pool of compounds produced by plants (Keppler et al., 2008). When isolated, these compounds have been shown to be precursors of methane under normal aerobic metabolism, although at very high temperatures (40 – 70 ºC). If plants can produce methane aerobically, an evaluation of which plants are producing methane and in what quantity is essential to understanding the global methane cycle.

The research described here had two main objectives: i) to investigate the influence of environmental factors on diurnal and seasonal patterns of methane flux from a natural fen in northern Alberta (the western peatland site of the Canadian Carbon Program research network), and ii) to determine what proportion of methane, if any, is being produced aerobically by *Sphagnum* moss, the predominant moss at the western peatland study site.

1 Mechanisms controlling diurnal and seasonal variation in methane fluxes from a northern Alberta peatland

1.1 Introduction

Boreal and sub-arctic peatlands are a major component of the soil carbon pool, containing approximately one-third (455 Pg) of global carbon stocks (Gorham, 1991; Post et al., 1982). The ability of peatlands to accumulate large quantities of carbon is due to relatively high rates of CO_2 sequestration coupled with low rates of decomposition associated with cold and anaerobic environments (Gore, 1983). In sequestering large quantities of CO_2, plants will deposit some carbohydrate to the anaerobic soil zone. These carbohydrates can then be metabolized to methane, an atmospheric gas having a greater global warming potential than CO_2 (Frolking et al., 2006; Roulet et al., 2007; Whiting and Chanton, 2001). Once methane is produced, some of it can be emitted to the atmosphere, where it can contribute to the greenhouse effect.

Much research has focused on identifying the environmental controls on seasonal variation in methane flux, with water table position (Moore and Roulet, 1993; Roulet et al., 1993), temperature (Alford et al., 1997; Crill et al., 1988; Heyer and Berger, 2000), and substrate availability (Christensen et al., 2003; Strom et al., 2003; Whiting and Chanton, 1993) all having an influence. Water table position will influence methane flux in a number of ways. The water table must be at a level where organic matter is within an anaerobic environment. If the water table is not at a level where

organic matter is within an anaerobic environment, methane production will not occur. Once a sufficient water table is met for methane production, changes in water table position will influence methane flux in two ways. First, a fluctuation in water table will either increase or decrease the anaerobic soil volume where methane production occurs. A higher or elevated water table will cause a larger soil volume for methane production, whereas a lowered table will cause a smaller soil volume for methane production. Secondly, fluctuations in water table depth will either increase or decrease the aerobic soil volume, where methane oxidation occurs. An increase in water table depth will increase the soil volume where methane oxidation occurs; where as a decrease in water table depth will decrease the soil volume where methane oxidation occurs. With a higher water table causing a larger soil volume for methane production and a smaller soil volume for methane oxidation, an increase in water table position is commonly associated with an increase in net methane emission to the atmosphere (Verma et al., 1992). Conversely, a decrease in water table position will cause a decrease in net methane emission to the atmosphere (Moore and Roulet, 1993; Roulet et al., 1993). Furthermore, water table depth can reach a point where the level of oxidation exceeds production, and there is a net influx of methane to the ecosystem (Roulet et al., 1993).

In addition to water table, methane flux will also be influenced by soil temperature. An increase in soil temperature will result in an increase in both methane production (Valentine et al., 1994; Zhuang et al., 2004) and oxidation (Einola et al., 2007; Visvanathan et al., 1999). Though increased soil temperature will influence both

methane production and oxidation, increases in soil temperature have been shown to increase net methane emission from peatlands (Alford et al., 1997; Crill et al., 1988; Hargreaves et al., 2001; Heyer and Berger, 2000; Macdonald et al., 1998; Sachs et al., 2008). Although multiple studies have found increased methane efflux with increased soil temperature, results differ in the observed relationship between temperature and methane flux. Past studies have shown an increase in soil temperature to result in a linear increase in net methane emission (Alford et al., 1997; Crill et al., 1988; Heyer and Berger, 2000; Macdonald et al., 1998), whereas other studies showed an increase in soil temperature to result in an exponential increase in net methane emission (Hargreaves et al., 2001; Macdonald et al., 1998; Sachs et al., 2008; Wille et al., 2008).

In addition to adequate soil temperature, as well as anaerobic soil conditions, substrate for methanogenesis must be present within soil in order for methane production to occur. Carbon substrates provide methanogenic microorganisms with molecules to metabolize in order to produce energy. Methane is then produced as a product of methanogenic metabolism. There are two types of substrate that can be utilized by methanogenic microorganisms, acetate (Wolfe, 1971) and CO_2 (Barker, 1936). Carbon dioxide will be present within the soil or peat from microorganism fermentation and other metabolic processes, where as acetate is formed from carbohydrate deposited by the root systems of wetland plants. Both CO_2 and acetate can serve as precursors for methane production (Barker, 1936; Schlesinger, 1997; Wolfe, 1971), where a higher supply of either can lead to an increase in methane

efflux. The rate of gross primary productivity (GPP) has been suggested as a proxy for the abundance of methanogenic substrate, where an increase in GPP was correlated to an increase in methane efflux (Bellisario et al., 1999; Whiting and Chanton, 1993). An increase in GPP would result in an increase in methanogenic substrate by photosynthesis causing the translocation of carbohydrate from leaves to the roots. Carbohydrate within the root can then exit the root to the soil through abrasions, and be converted to acetate which can be used by methanogenic microorganisms.

In addition to research into seasonal variation in methane flux, diurnal cycles have been studied. Previous studies have attributed diurnal cycles in methane flux to correlated temperature changes (Alford et al., 1997; Seiler et al., 1984; Zhu et al., 2007), variation in stomatal opening and closing (Garnet et al., 2005; Hirota et al., 2004; Morrissey et al., 1993; Yavitt et al., 2006), shifts in substrate availability (Wang and Han, 2005) and changes in pressurized bulk flow through plants (Sebacher et al., 1985; Whiting and Chanton, 1996). Stomatal opening and closing, and pressurized bulk flow will influence diurnal trends in methane flux in wetland plants such as *Carex* spp. and *Typhia* spp. which can act as conduits for methane movement from the anaerobic rhizosphere to the atmosphere (Chanton and Dacey, 1991; Cicerone and Oremland, 1988). These wetland plants act as a conduit by having a specialized plant tissue termed aerenchyma (Sachs, 1882), used to aid the diffusion of oxygen to water-logged root zones (Armstrong and Armstrong, 1991; Armstrong, 1978; Armstrong, 1979; Nouchi et al., 1990). Methane can diffuse into

plant root aerenchyma from the soil and diffuse through the plant to be emitted to the atmosphere (Chanton and Dacey, 1991; Cicerone and Oremland, 1988), as oxygen diffuses from the atmosphere to roots. Previous studies have shown that stomatal opening (Hirota et al., 2004; Morrissey et al., 1993) and pressurized bulk flow (Chanton et al., 1993; Whiting and Chanton, 1996) can influence the rate that methane is released from the plant. Variation in stomatal conductance will influence methane flux by either allowing more diffusion of methane from leaves with stomata opening or restricting methane diffusion from leaves with stomatal closure. Pressurized bulk flow of gases is driven by pressure gradients within plants, caused by higher pressure created in young leaves. An increase in pressure will occur within young leaves because of higher temperature (Dacey, 1981a; Dacey, 1981b) and differences in relative humidity (Armstrong and Armstrong, 1991) in comparison to other plant organs. This increased pressure will force gases present within young leaves through the stem and into root systems (Dacey, 1981b). As gas is forced from young leaves throughout the plant, gases within roots and stems will vent out of old and broken stems. Pressurized bulk flow will increase the rate that gases move through plants when compared to diffusion (Armstrong and Armstrong, 1990; Armstrong and Armstrong, 1991; Dacey, 1981a; Dacey, 1981b). Some plants have been shown to switch from gas diffusion at night, to pressurized bulk flow during the day, resulting in higher methane flux during the day (Whiting and Chanton, 1996). Also, the controls on pressurized bulk flow will vary diurnally, which can result in a diurnal cycle in methane flux. A diurnal trend in methane flux has been shown in ecosystems where plants influence methane flux (Chanton et al., 1993; Whiting and

Chanton, 1996). However, it has been debated whether stomatal regulation or pressurized bulk flow are responsible for these diurnal trends, with evidence supporting stomatal control (Hirota et al., 2004; Morrissey et al., 1993) and some other evidence supporting pressurized bulk flow control (Chanton et al., 1993; Whiting and Chanton, 1996).

Some of the mechanisms contributing to diurnal and seasonal variation in methane flux have been well documented, but recently new studies have suggested that atmospheric turbulence can also influence methane flux (Fan et al., 1992; Sachs et al., 2008; Wille et al., 2008). Atmospheric turbulence will increase the rate that dissolved methane diffuses from surface water, resulting in a higher flux to the atmosphere (MacIntyre et al., 1995). An increase in methane flux from water occurs because turbulence increases methane transfer velocity across an aqueous boundary layer at the water/air interface (MacIntyre et al., 1995). The aqueous boundary layer can often limit the diffusion of methane; therefore, an increase in the transfer velocity of methane across this layer will cause methane flux from water to air to increase. Turbulence will also directly influence methane flux by thinning the laminar boundary layer at the soil surface. As the laminar boundary layer is thinned, a higher concentration gradient of methane between soil and air is created, thus increasing diffusive flux of methane from soil. Lastly, higher turbulence will influence methane flux indirectly by perturbing vegetation that methane bubbles are adhered to (Sachs et al., 2008; Wille et al., 2008). As vegetation is perturbed, more methane bubbles will be released resulting in an increase in methane flux from the area of shifted

vegetation. The observations of Wille et al. (2008) and Sachs et al. (2008) were consistent with previous studies conducted on CO_2 exchange within marine ecosystems, where turbulence was shown to be an important control on CO_2 flux from water (Wanninkhof and McGillis, 1999). Wille et al. (2008) and Sachs et al. (2008) showed that changes in turbulence can influence seasonal variation in methane flux, but turbulence can also vary diurnally, with peak turbulence commonly occurring during the day and minimum levels of turbulence occurring at night. If turbulence is a control on methane flux, diurnal trends in turbulence should have an impact on diurnal trends of methane flux.

The evaluation of mechanisms controlling diurnal and seasonal variation in methane flux is important because of the role of methane emission from the peatlands on the greenhouse gas budget of the atmosphere. When present within the atmosphere, methane acts as a radiative forcing agent, capturing and re-emitting long wave radiation, which results in warming of the earth's surface. The ability to capture and re-emit long wave radiation is a property held by all greenhouse gases, but each greenhouse gas has a different efficiency in doing so, termed radiative forcing efficiency (IPCC, 2001; Shine and Forster, 1999). A higher radiative forcing efficiency means more radiative forcing per molecule. Compared to CO_2, methane has a higher radiative forcing efficiency, thus, a mole of methane present within the atmosphere contributes more to greenhouse warming than a mole of CO_2 present in the atmosphere (IPCC, 2001). With peatlands emitting methane and sequestering CO_2, a comparison can be made between methane and CO_2, to determine if a

peatland is acting as a net sink or source of radiative forcing agents (Friborg et al., 2003; Frolking et al., 2006; Roulet et al., 2007; Whiting and Chanton, 2001). In order to compare CO_2 and methane, methane flux values must first be scaled to CO_2 equivalents (IPCC, 2001; Whiting and Chanton, 2001). Once methane flux is converted to CO_2 equivalents, a direct comparison can be made between fluxes of methane and CO_2, to determine if the peatland is acting as a net sink or source of radiative forcing agents (Friborg et al., 2003; Frolking et al., 2006; Whiting and Chanton, 2001).

Here I present a study of net methane flux, measured by eddy-covariance, in a northern Alberta peatland. This study had three objectives: i) To assess how turbulence, incoming shortwave radiation, and soil temperature influence diurnal cycles in methane flux, ii) to assess how changes in soil temperature, GPP, capacity for methane emission and water table position influenced seasonal trends in methane flux, and iii) to determine if the peatland was acting as a net source or net sink of radiative forcing agents. A clear diurnal pattern in methane flux was found with peak fluxes measured during daytime hours and minimum fluxes measured at night. These cycles were correlated with diurnal cycles in soil temperature and shortwave radiation. In addition to diurnal cycles, a seasonal variation in net methane emission was observed, with peak flux measured in July. Seasonal variation in net methane emission was explained through changes in soil temperature and calculated seasonal changes in the capacity for net methane emission (respiration) at 10 ºC (R_{10}).

1.2 Methods

1.2.1 Study site description

The study was conducted at the western peatland of the Canadian Carbon Program (formerly Fluxnet Canada), which is located approximately 80 km northeast of Athabasca, Alberta (58.2 ºN, 113.52 ºW).The western peatland is classified as a "moderately-rich treed fen" (Vitt et al., 1998), with above ground vegetation dominated by stunted *Picea mariana* and *Larix laricina* trees. The site also has populations of moss (*Sphagnum* spp., *Drepanocladus aduncus, Pleurozium schreberi*), shrub (*Betula pumila, Salix* spp.), dwarf shrub (*Andromeda polifolia*,) and herb species (*Carex* spp., *Menyanthes trifoliata*) (Syed et al., 2006).

The thirty-year mean annual temperature (1971-2000) was 2.1 ºC, with a mean growing season (May - October) temperature of 11.7 ºC. Long-term average annual precipitation (1971-2000) was 504 mm, with 360.5 mm falling within the growing season. Of the 504 mm of precipitation, 122 mm was in the form of snow, with the remaining 382 mm being rain (Environment Canada, 2004). The long-term average temperature and precipitation were measured in Athabasca, Alberta, which is approximately 80 km from the western peatland flux station. For a more complete description of the study site see Syed et al. (2006).

1.2.2 Meteorological measurements

Measurements of precipitation, air temperature, peat temperature, soil moisture content and water table depth were collected throughout the 2007 growing season. Air temperature was measured with a temperature and relative humidity probe (HMP45C (Vaisala Inc.), Campbell Scientific) located within a ventilated radiation shield (MetOne, Campbell Scientific) installed above the tree canopy, 5 m above ground. In addition, two platinum resistance thermometers were installed within the radiation shield to measure air temperature. Shortwave radiation was measured by a four-component net radiometer (CNR1, Kipp & Zonen, Delft, The Netherlands) located on a 6 m tall tower, 15 m from the flux tower. Soil temperature was measured by thermistors (107B Soil Temperature Probe, Campbell Scientific) in two profiles, one in a hummock and one in a hollow at 6 successive depths of 2, 5, 10, 20, 50 and 100 cm. An average of the 50 cm hummock soil temperature and the 20 cm hollow soil temperature was used as a best estimate of soil temperature within the zone of methane production. The zone of methane production was expected to be associated with the position of the water table, with the assumption that peat and soil below the water table surface was under anaerobic conditions. An average of the 50 cm hummock soil temperature and 20 cm hollow soil temperature was used to characterize the soil zone of methane production because both temperature measurements were close to the water table surface. These measurement points for temperatures were both close to the water table surface because of the different vertical positions used as reference points for the hummock and hollow soil profiles. The peat surface at a hummock was further from the water table (higher in elevation)

than the peat surface at a hollow, therefore soil temperature probes inserted within a hummock were further from the water table than soil temperature probes inserted within a hollow. The difference between the peat surface of the hummock and the hollow was approximately 30 cm, therefore the 50 cm hummock soil depth and 20 cm hollow soil depth, were located approximately at the same vertical position within the peat. All references to soil temperature in the remainder of this manuscript refer to an average of the 50 cm hummock soil temperature and the 20 cm hollow soil temperature. Soil moisture was measured with soil water content reflectometers (CS616-L, Campbell Scientific), installed at depths of 7.5, 10 and 12.5 cm below the peat surface. The reflectometers had previously been calibrated in the lab in moss peat held at a range of water contents. Water table depth was measured through the use a float and counter-weight system, connected to a potentiometer. The float and potentiometer were mounted within a perforated PVC pipe that was anchored within the clay layer underlying the peat. Perforations at the bottom of the PVC pipe allowed the entrance of water, and water table position was represented by the vertical position of water level within the pipe. Water table depth was referenced to the average hummock height within a 2 m radius of the PVC pipe. All meteorological data except precipitation, were collected by a datalogger (CR23X, Campbell Scientific) located within the instrumentation hut. Sensors were scanned at 5-second intervals and averages recorded at 30-minute intervals, 24-hours a day. Precipitation was measured with a weighing rain gage (T-200B, Geonor Inc., The Netherlands) located 800 m from the instrumentation hut. Precipitation data were collected by a datalogger (CR10, Campbell Scientific) located within an instrument box near the

base of the Geonor rain gauge. Precipitation measurements were made every 5 seconds, with 30-minute cumulative totals recorded 24-hours a day.

1.2.3 Flux measurements

Methane flux measurements were made using the eddy covariance technique (Aubinet et al., 2000; Baldocchi et al., 1988; Moncrieff et al., 1997). This required simultaneous measurements of vertical wind speed and methane concentration in air. To measure wind direction and speed, a sonic anemometer-thermometer (CSAT3, Campbell Scientific, Logan, Utah, USA) was mounted atop a 9 m mast, and positioned into prevailing winds (west). Methane concentrations were measured by a tunable diode laser absorption spectrometer (TDLAS) (TGA100A, Campbell Scientific, Logan, Utah). The TGA100A consisted of a hard shell housing, liquid nitrogen dewar, laser, sample cell, reference cell, reference and sample detectors, and an onboard computer. For a more complete overview of the TGA100A see Billesbach et al. (1988). The TGA100A measured infrared radiation absorption at a waveband of 3018.53 cm^{-1}, which is specific to CH_4. Infrared radiation having a wavelength of 3018.53 cm^{-1} was produced by the laser, which was maintained at a temperature of 82.3 ºK. The sample and reference cells were temperature regulated at 29 ºC by heaters within the hard shell housing and each cell was maintained under a constant pressure of ~ 50 mbar. Sample and reference detectors were temperature controlled and were maintained at -28 and -25 ºC, respectively. The reference cell was flushed with air continuously having a methane concentration of 2 %. The measurement conditions described above were held constant throughout the entire sampling period.

The TGA100A was positioned at the base of the mast, on a 1.5 m x 3 m wood platform. The TGA100A and platform were shielded from rain and sun by a non-transparent, waterproof roofing. A sample intake was mounted atop the 9 m mast, positioned 15 cm away from the transducers on the sonic anemometer. Air was pulled from the sample tube inlet to the TGA100A by a rotary-vane vacuum pump (RB0021, Busch Inc., Virginia Beach, Virginia, USA), at a flow rate of 17 L min^{-1}. Connected to the ½" outside diameter sample tubing (Synflex Hose and Tubing Products, Fairfield Ohio) was a high capacity Nafion® (Perma Pure Inc., Toms River, New Jersey, USA) sample dryer (PD1000, Campbell Scientific, Logan, Utah, USA), used to dry the sample air prior to analysis. The sample tube was equipped with two filters, one stainless steel filter (15 µm) located at the inlet of the sample tube and one paper filter (1 µm) located at the inlet of the Nafion drier, to remove airborne dust from the sample. Filters were changed at regular intervals of approximately 30 days. A delay of 0.9 seconds occurred from the time air entered the sample intake, to response of the TGA100A. Methane concentration, wind speed and wind direction measurements of the sonic anemometer were recorded at 10 Hz by a CR5000, saved on a data card (Campbell Scientific, Logan, Utah, USA). Methane flux and methane air column storage data were processed within MATLAB (The Mathworks Inc., 2006), allowing the calculation of 30-minute averages of net ecosystem methane flux. A positive sign convention indicated net efflux of methane from the peatland and a negative sign convention indicated net influx of methane to the peatland.

Bi-weekly calibrations of the TGA100A were conducted. The TGA100A performance was evaluated in two ways. First, we evaluated TGA100A measurements of absolute concentration of two known calibration gases (Figure 1.1; Table 1.1). In addition to bi-weekly calibration checks, measured CH_4 concentration data were compared to CH_4 concentration measurements recorded simultaneously by Environment Canada using independent instruments at the site (Figure 1.2). The comparison between the TGA100 methane concentration data and the Environment Canada methane concentration data, allowed for a rigorous check on the quality of the TGA100A methane concentration measurements.

Carbon dioxide, water vapour and sensible heat flux measurements were also made with the eddy covariance technique (Aubinet et al., 2000; Baldocchi et al., 1988; Moncrieff et al., 1997) using additional independent measurements. The CO_2, water vapour and sensible heat eddy covariance system consisted of a sonic anemometer (SAT, Solent R3, Gill Instruments Ltd., Lymington, England) to measure wind direction, wind speed and sonic air temperature, and a fast response infra-red gas analyzer (IRGA; LI7000, LI-COR, Lincoln, Nebraska, USA) to measure CO_2 and water vapour concentration. Water vapour flux measurements were then used to calculate ecosystem conductance as:

$$G = \frac{\left(\frac{\lambda E}{44000}\right)}{\left(\frac{VPD}{P}\right)} \qquad (1)$$

where:

G = ecosystem conductance (mol m^{-2} s^{-1})
λE = latent heat flux (W m^{-2})
VPD = vapour pressure deficit (kPa)
P = atmospheric pressure (kPa)

For a more complete description of the second eddy covariance system used at this site see Syed et al. (2006).

1.2.4 Data screening

In order to obtain reliable measurements of flux with the eddy covariance technique, flux data must be screened to remove data from time periods with inadequate turbulence. Friction velocity (u^*) was used as a measure of turbulence. Methane flux data was screened using three different approaches. In the first approach, all methane flux values recorded when u^* was less than 0.15 m s^{-1} were removed. The threshold value of 0.15 m s^{-1} was selected because it was shown to be an appropriate value at this site for net ecosystem CO_2 flux data (Syed et al., 2006). The second u^* screening method removed all methane flux data with a corresponding u^* less than 0.18 m s^{-1}. The second u^* threshold value of 0.18 m s^{-1} was selected based on an analysis evaluating the relationship between u^* and methane flux, with data averaged over the entire growing season (Figure 1.3). To conduct an analysis of u^* and methane flux, methane flux measurements and the associated u^* values (rank ordered) were split into ten separate groups, with each group representing 10 % of the data set. The average u^* and average methane flux of each group was then calculated and plotted to evaluate the relationship between methane flux and u^* (Figure 1.3). I selected a

threshold value of 0.18 $m\,s^{-1}$ because it was the u^* value above which no significant change occurred in methane flux values (approximately a zero slope for the relationship between u^* and methane flux). The third and final approach involved selecting separate u^* thresholds for each month. The following values of 0.21, 0.18, 0.23, 0.28 and 0.21 $m\,s^{-1}$ were selected for May, June, July, August and September, respectively, for the 2007 growing season. A separate u^* threshold value for each month was determined based on the relationship between u^* and methane flux within each individual growing season month (Figure 1.4) as described above. Using data from the month of May, I was unable to determine a u^* threshold value due to high variance in the limited data set. To screen data in May, I used the same u^* threshold as was used in September. I used the September u^* threshold for May because of all months within the 2007 growing season, May and September had the most similar trends in methane flux. For all months other than May, the u^* threshold value was selected as the u^* value above which the slope of the relationship between methane flux and u^*, was approximately zero or not significantly different from zero.

1.2.5 Global warming potential calculations

A comparison between net CO_2 influx and net CH_4 efflux was made for the western peatland in the 2007 growing season. The purpose of this comparison was to determine if the western peatland was acting as a net source, or sink of greenhouse gases. The integrated fluxes of CH_4 and CO_2 were calculated for each month, with a coefficient applied to CH_4 flux in order to account for a larger warming effect of CH_4, when present within the atmosphere. In addition, three time horizons were

considered: 20, 100 and 500-years, which referred to the residence time of sequestered CO_2 within peat or soil. For example, a time horizon of 500 years, refers to sequestered CO_2 remaining within peat or soil for 500 years. A coefficient of 21.8, 7.6 and 2.6 was applied to methane flux data, for the 20, 100 and 500 year time horizons, respectively (Whiting and Chanton, 2001). The application of coefficients is to equate methane to CO_2, in terms of radiative forcing capacity. With the application of these coefficients, methane was then expressed in units of CO_2 equivalents, which allowed a direct comparison between methane emission and CO_2 sequestration. The NEE in CO_2 equivalents were represented as:

$$NEE_{CO_2 equivalents} = NEE\ CO_2 + NEE\ CH_4 \bullet th_c \quad (2)$$

where:

NEE CO_2 = net ecosystem exchange of CO_2 (mol m^{-2} $month^{-1}$)
NEE CH_4 = net ecosystem exchange of CH_4 (mol m^{-2} $month^{-1}$)
th_c = selected coefficient for a particular time horizon

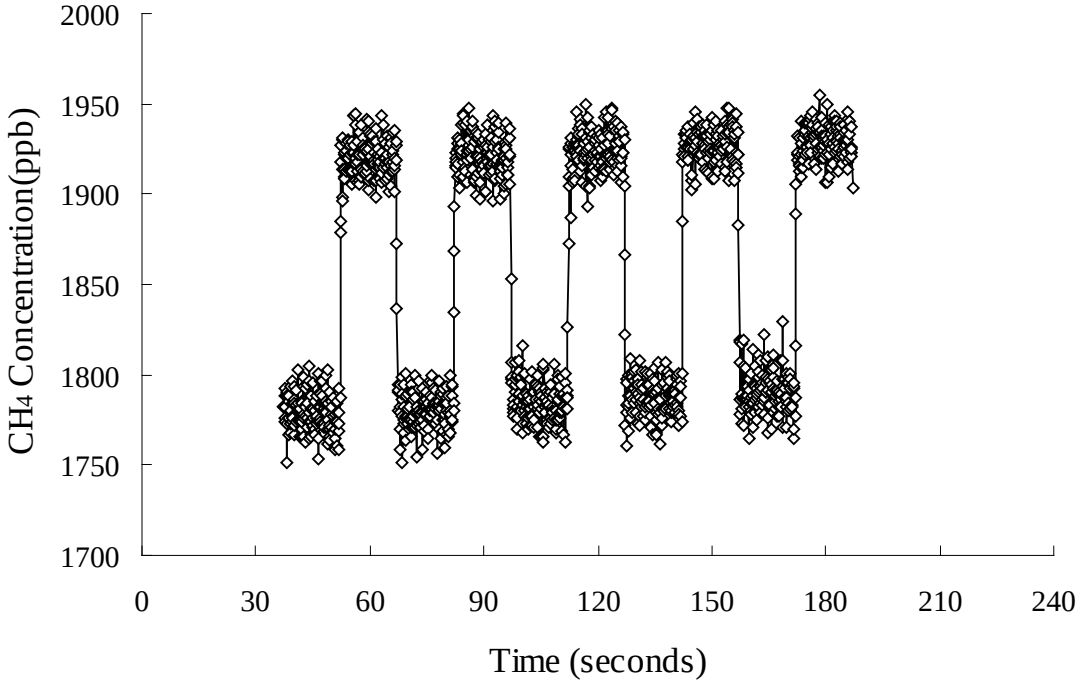

Figure 1.1: An example calibration performed on July 25, 2008, for the TGA100A at the western peatland flux station in northern Alberta. Calibrations were performed in order to assess the accuracy of the TGA100A in determining the difference of CH_4 concentration between a calibration gas having a concentration of 1745 ppb and a second calibration gas having a concentration of 1884 ppb. The TGA100A accurately measured this difference correctly for every calibration throughout the 2007 growing season although there was some drift in the absolute concentration values (see Table 1.1 for additional information related to this calibration test).

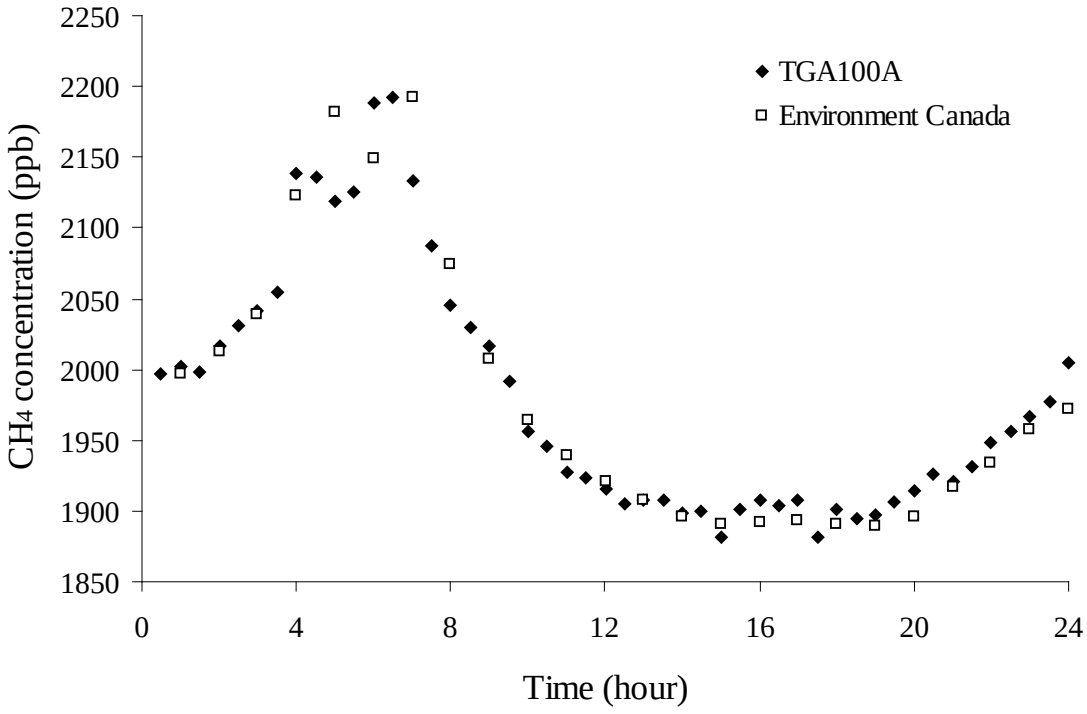

Figure 1.2: A comparison between the TGA100A and Environment Canada methane measurements performed on bin-averaged July 2007 data, at the western peatland flux station in northern Alberta. These results are typical for other comparisons throughout the growing season.

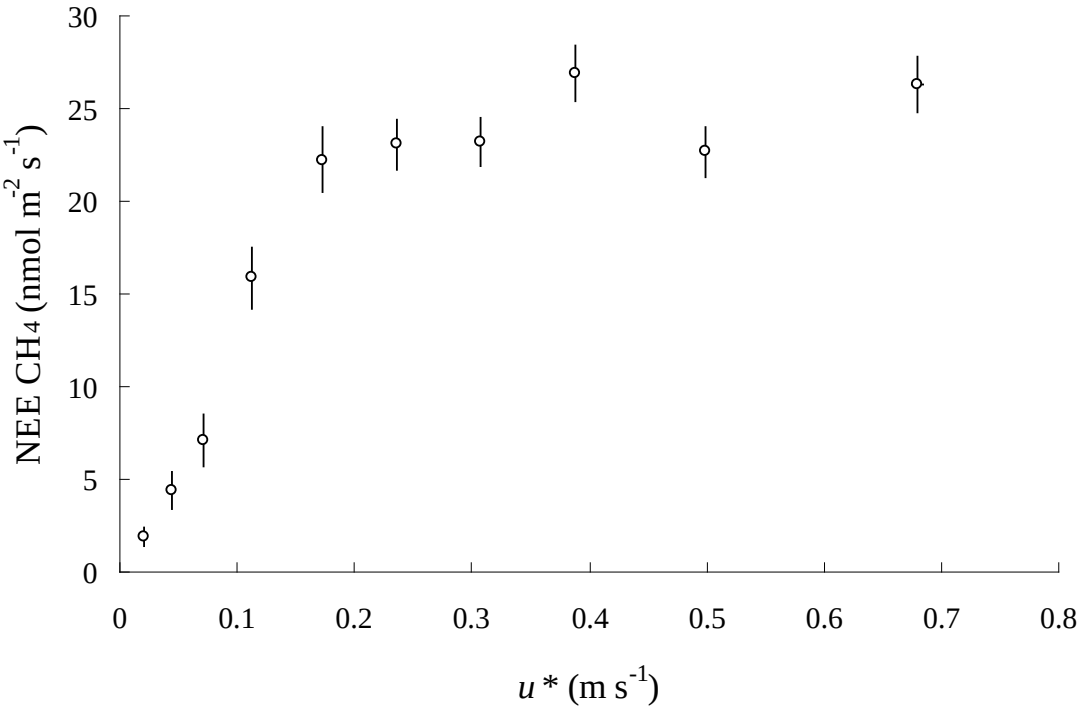

Figure 1.3: The relationship between friction velocity (u^*) and NEE CH_4 for the entire 2007 growing season. Data were rank ordered and grouped by u^*, with each data point representing 10 % (n = 467) of the total methane flux data. The average u^* ± SEM (error bars do not exceed the width of data labels) and average NEE CH_4 ± SEM is presented for each group.

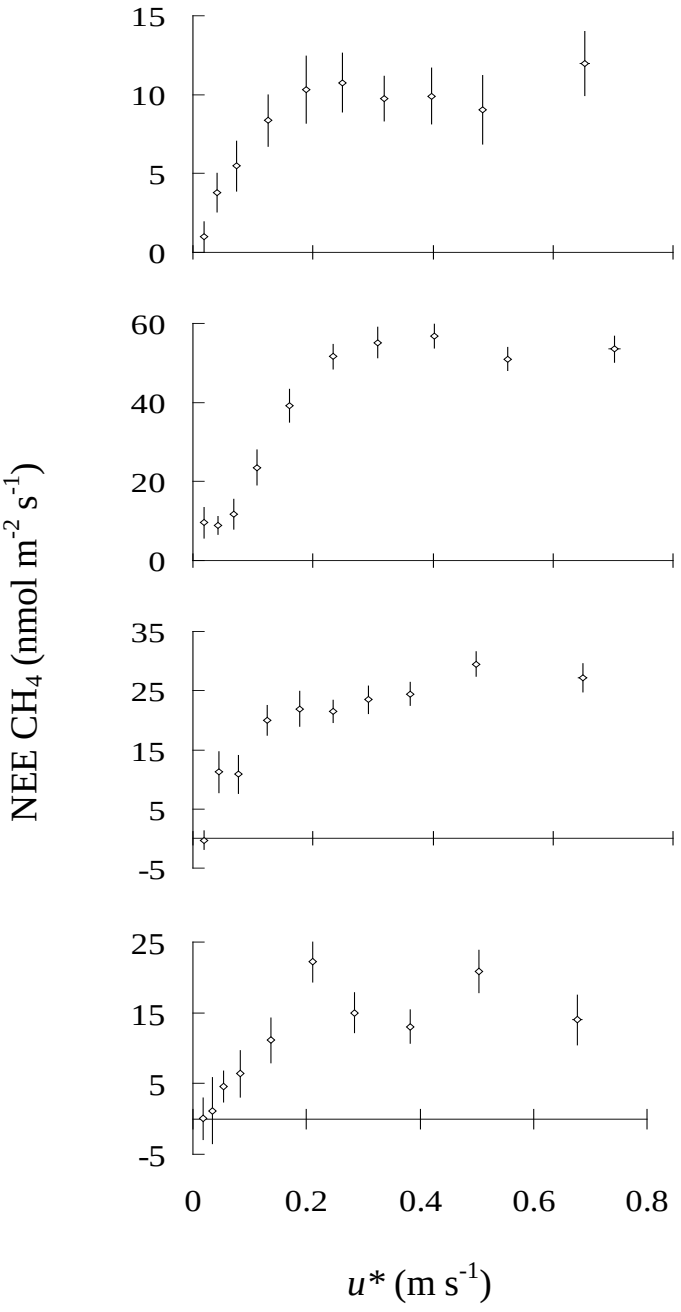

Figure 1.4: The relationship between average friction velocity (u^*) ± SEM and average NEE CH_4 ± SEM for June (top graph), July (second from top graph), August (second from bottom graph) and September (bottom graph) of the 2007 growing season. Each data point represents 86, 99, 120, and 89 u^* and methane flux measurements (10 % of methane flux data) for June, July August and September, respectively.

Table 1.1: An example calibration performed on July 25, 2008, for the TGA100A at the western peatland flux station in northern Alberta. Calibrations were performed in order to assess the accuracy of the TGA100A in determining the difference of CH_4 concentration between a calibration gas having a concentration of 1744.7 ppb and a second calibration gas having a concentration of 1884.3 ppb. The TGA100A accurately measured this difference correctly for every calibration throughout the 2007 growing season.

Injection	Standard 1 CH_4 Conc. (ppb)	Standard 2 CH_4 Conc. (ppb)
1	1777.8 ± 10.5	1919.6 ± 9.2
2	1781.1 ± 9.6	1920.3 ± 11.0
3	1782.9 ± 10.3	1925.1 ± 10.3
4	1786.9 ± 9.5	1927.6 ± 9.8
5	1790.3 ± 10.4	1928.6 ± 9.6
Observed (Average ± SD) n = 5	1783.8 ± 4.9	1924.3 ± 4.1
Standard	1744.7	1884.3
Difference (Obs - Std)	39.1	40.0

1.3 Results

1.3.1 Seasonal variation in temperature, precipitation, water table depth and soil moisture

Throughout the 2007 growing season, high seasonal variation in precipitation was observed (Figure 1.5). June had the highest cumulative rainfall with October displaying the lowest cumulative rainfall. July was uncharacteristically dry, with observed 2007 values approximately 65 millimeters lower than the 30-year average (1971 - 2000). Precipitation in May, June, August and September were all similar to the long-term average precipitation, with all monthly values within one standard deviation of the respective 30-year means. In contrast, July and October each displayed monthly precipitation values lower than the long-term average precipitation (1971 - 2000), with both falling greater than one standard deviation below the long-term mean.

Large variation in monthly average air temperature was displayed through the 2007 growing season, with the highest mean monthly temperature being observed in July and the lowest mean monthly air temperature being observed in October (Figure 1.7). May, June, September and October all had average temperatures near the long-term average, all falling within one standard deviation of the long-term mean for each respective month (1971 - 2000). In contrast, mean temperature in July exceeded the long-term average temperature for the month. Also, average temperature in August

fell greater than one standard deviation below the 30-year respective mean (1971 - 2000). Variation in air temperature resulted in changes in soil temperature. Like air temperature, soil temperature had a peak monthly average value in July (Figure 1.7). In contrast, the lowest monthly average soil temperature was recorded in May.

Seasonal variation in air temperature displayed a daily maximum exceeding 10 ºC from late May to late September, with peak values (>30 ºC) observed in July (Figure 1.8 a). Daily minimum air temperature remained above freezing for a brief period from mid-June to mid-August. The lowest daily minimum air temperature, of nearly -10 ºC, was observed in October of the 2007 growing season (Figure 1.8). The temperature buffering affect of the overlying peat resulted in a decrease in daily temperature fluctuation within soil. Decreased temperature fluctuation within soil was displayed through a small difference between daily maximum soil temperature and daily minimum soil temperature (Figure 1.8).

The reduced daily variation in temperature within soil was also displayed through an evaluation of diurnal fluctuation in soil temperature. A diurnal cycle in temperature was observed within air and soil, over the entire growing season (Figure 1.9). Maximum air temperature occurred in the mid afternoon (16:00), with minimum air temperature occurring in the early morning (4:30). Maximum soil temperature occurred in the early evening (17:30), with minimum soil temperature being displayed in the mid-morning (6:30). The magnitude of diurnal change in air temperature (difference between maximum and minimum daily temperatures) was

10.7 ºC over the entire growing season (Figure 1.9). Diurnal variation in soil temperature was much less than that observed in air, with the difference between daily maximum and minimum values being only 1.7 ºC. A second evaluation of diurnal cycles in temperature was conducted comparing daytime and nighttime values. Daytime was defined as any period where photosynthetic photon flux density (PPFD) was greater than 50 µmol m^{-2} s^{-1} and nighttime as any period where PPFD was less than 50 µmol m^{-2} s^{-1}. This value was selected because during nighttime periods, PPFD did not exceed 50 µmol m^{-2} s^{-1} and during daytime periods PPFD did not fall below 50 µmol m^{-2} s^{-1}. Within air, daytime temperatures were higher than nighttime temperature in every month of the growing season (Figure 1.10). In contrast, daytime soil temperatures did not differ from nighttime soil temperature for May, June and July. However, in August and September, daytime average soil temperature exceeded nighttime average soil temperature by 1 and 0.74 ºC, respectively (Figure 1.10).

Seasonal and daily variation in temperature and precipitation will influence other abiotic processes such as soil moisture and water table depth. An increase in temperature resulted in high rates of evaporation which caused soil moisture reduction and water table draw down, with inputs of precipitation causing an increase in soil moisture and water table position. Soil moisture remained relatively constant early in the 2007 growing season (Figure 1.11). After the relatively constant soil moisture of the early season, two different periods characterized by soil moisture reductions were observed (Figure 1.11). Early in July, a rapid decrease in soil

moisture was displayed coinciding with a period of low precipitation and warm temperature. After this rapid decrease in soil moisture, a moderate reduction in soil moisture occurred throughout the remainder of the growing season (Figure 1.11). The 2007 growing season displayed substantially lower soil moisture values than a typical growing season as represented by 2005. 2005 was considered to be a typical growing season for soil moisture content because monthly precipitation and temperature both displayed values close to the 30-year average (1971-2000), measured in Athabasca, AB (80 km away). With temperature and precipitation being two of the major controlling factors of soil moisture content, 2005 moisture levels were regarded as a good estimate of the long-term average soil moisture content.

The water table position remained relatively stable early in the 2007 growing season, after which a decreasing trend in water table position was observed (Figure 1.12)**.** There was a sharp increase in water table depth for the second half of July, continuing until early August. This decrease occurred throughout a period of warm temperatures and reduced precipitation. The water table position for the 2007 growing season was substantially lower than what was considered a long-term average water table, as represented by 2005. A long-term average water table was inferred in the same manner as was soil moisture levels, with both being controlled by precipitation and temperature.

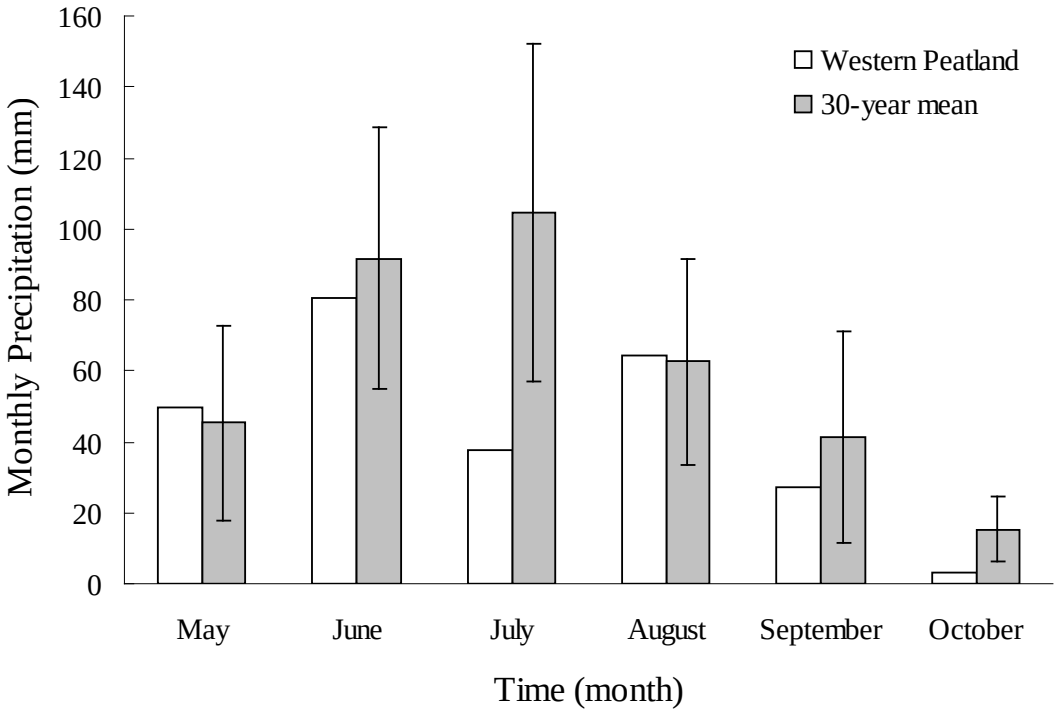

Figure 1.5: A comparison of the cumulative monthly precipitation measured at the western peatland flux station for the 2007 growing season, and the long-term monthly (30-year) average precipitation ± SD measured at Athabasca, Alberta.

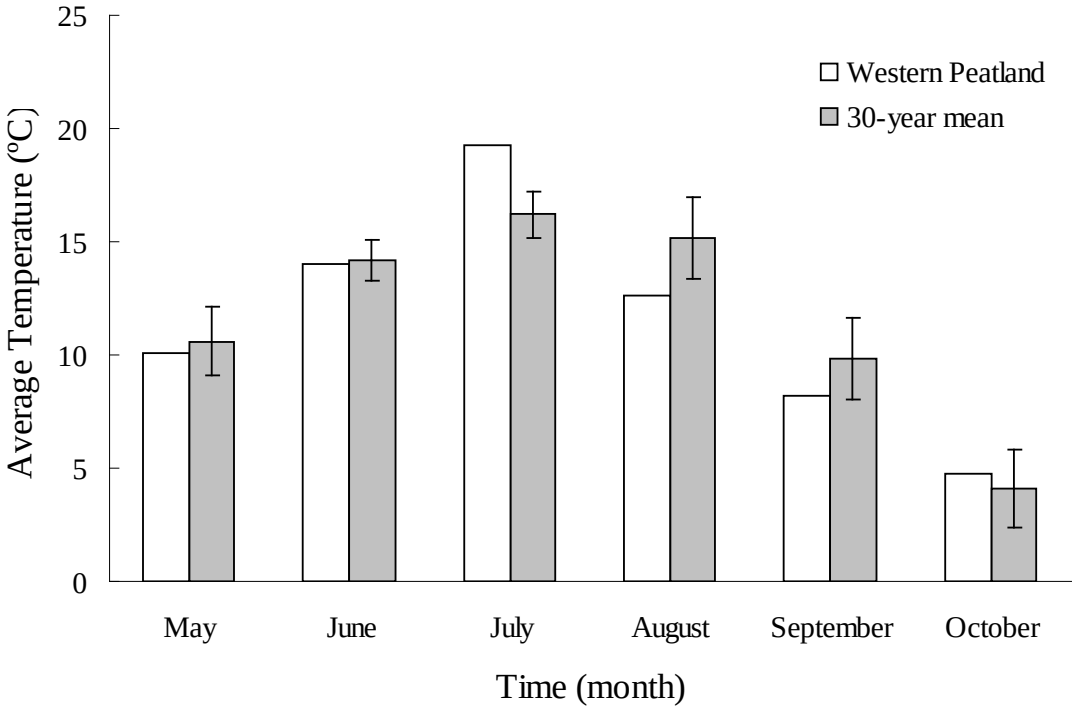

Figure 1.6: An evaluation of the mean monthly air temperature measured at the western peatland flux station. Monthly air temperature was compared with long-term monthly (30-year) average temperature ± SD measured at Athabasca, Alberta.

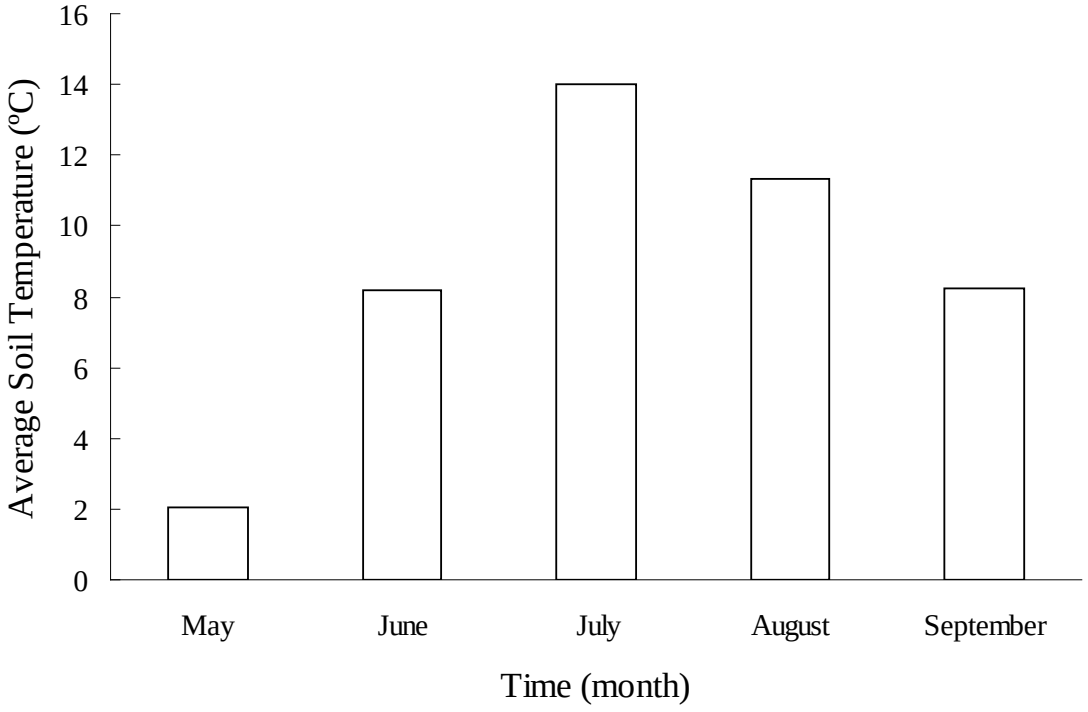

Figure 1.7: The average monthly soil temperature for each month of the 2007 growing season. All measurements were taken at the western peatland flux station, in northern Alberta.

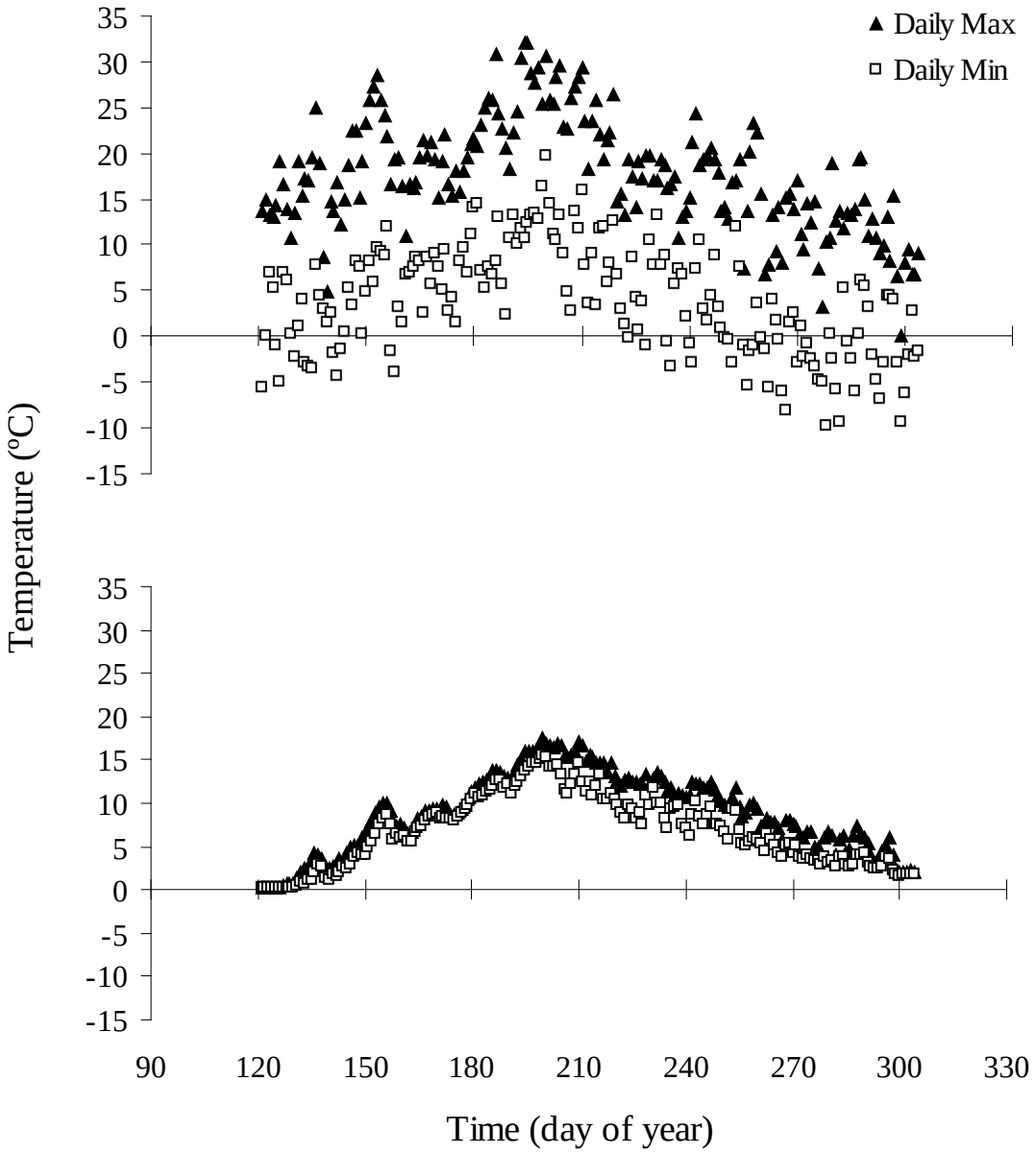

Figure 1.8: A comparison of the daily maximum and daily minimum temperature for air (upper graph) and soil zone of methane production (lower graph). The temperature within the soil zone of methane production was the average of temperature measurements taken at a 50 cm hummock peat depth and a 20 cm hollow soil depth.

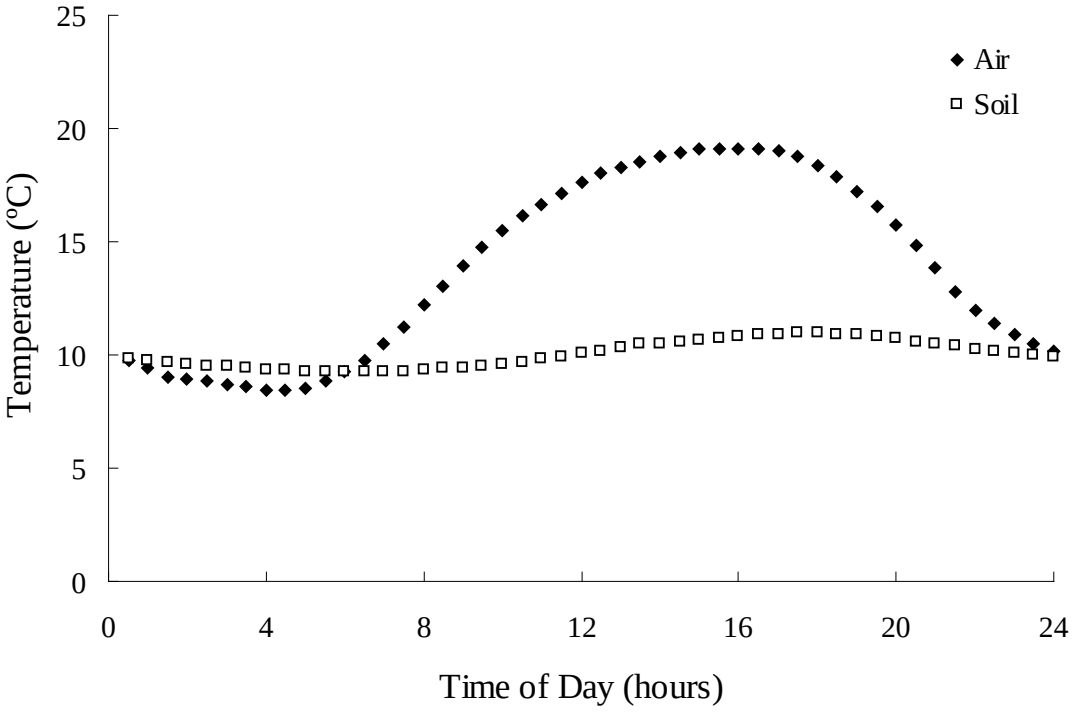

Figure 1.9: The diurnal cycle in air temperature and soil temperature within the zone of methane production (average of 20 cm hollow & 50 cm hummock) for the entire 2007 growing season.

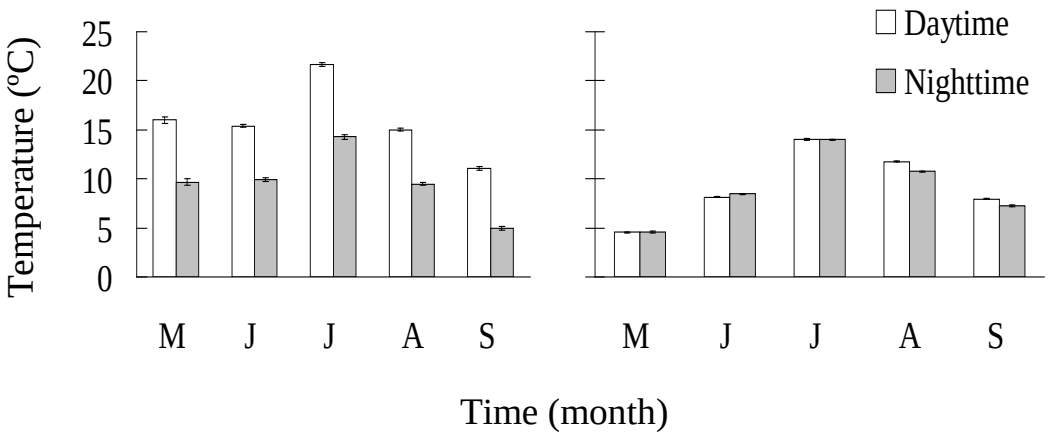

Figure 1.10: The average daytime and nighttime temperature of air ± SEM (left column) and 20 cm soil and 50 cm soil temperature ± SE (right column) for each month of the 2007 growing season. All measurements were taken at the western peatland flux station in northern Alberta.

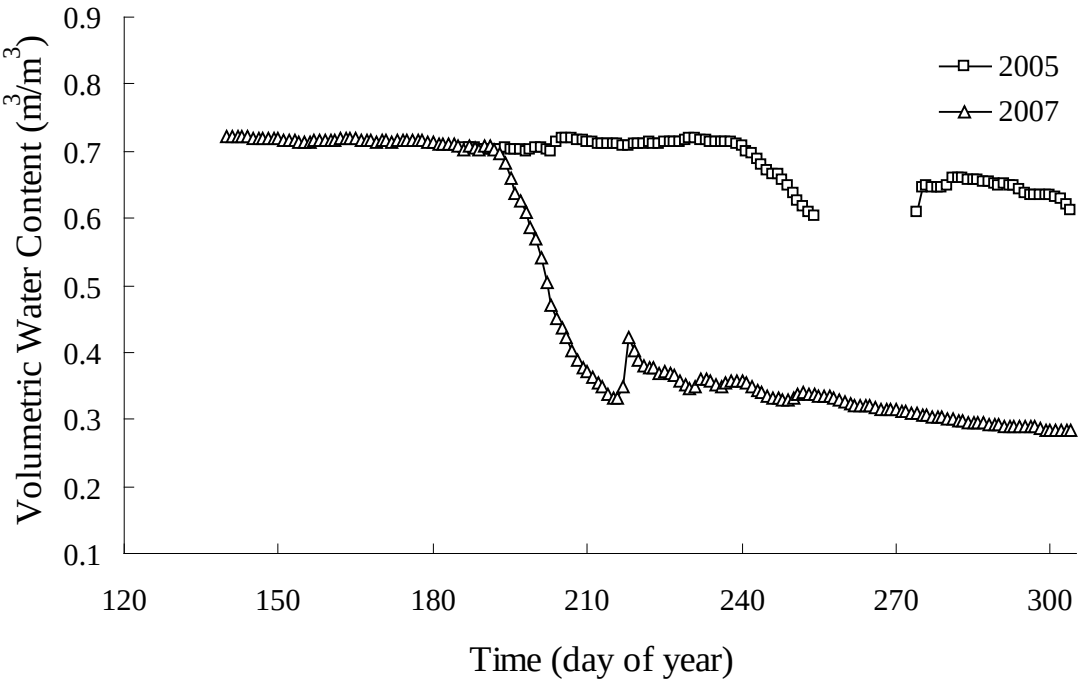

Figure 1.11: A comparison of volumetric water content within peat for two years, 2005 and 2007, at the western peatland flux station, in northern Alberta. Volumetric water content was measured at 3 depths (7.5, 10, 12.5 cm below hollow) and the average moisture of all three depths plotted.

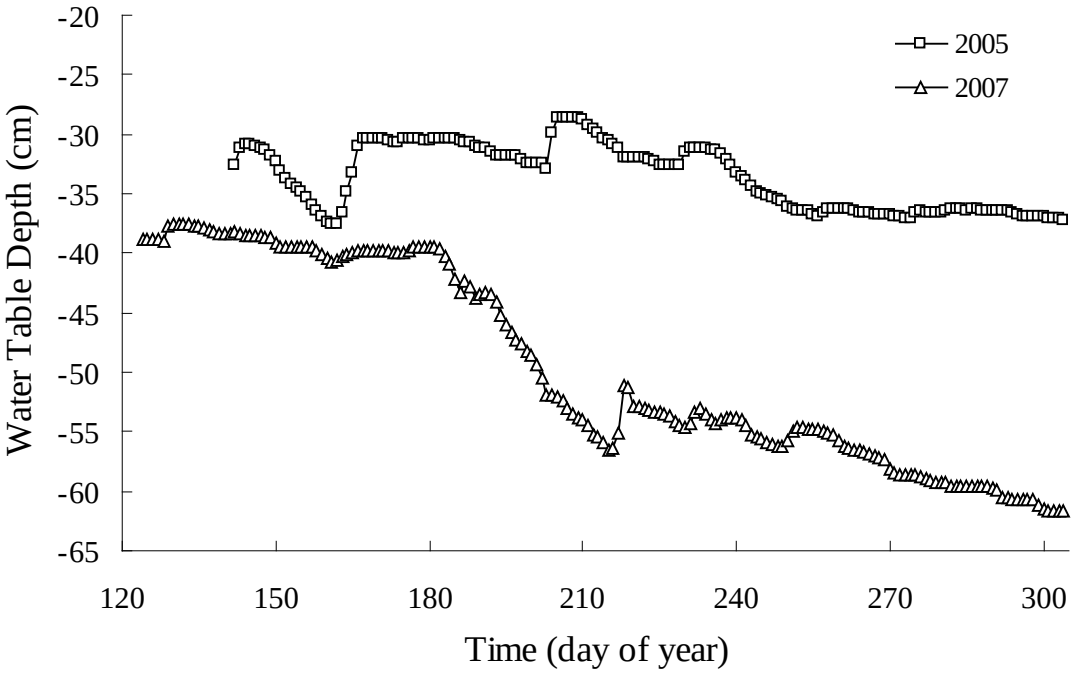

Figure 1.12: A comparison of the water table depth for two years, 2005 and 2007, at the western peatland flux station, in northern Alberta. Values represent the depth of water below the average hummock height.

1.3.2 Diurnal, monthly and seasonal methane flux trends under different u* screening methods

A significant diurnal pattern in methane flux (Table 1.2) and *u** (Table 1.3) was observed under every *u** screening, for the 2007 growing season. Early morning and evening were characterized by low methane flux and low *u**, while late morning and early afternoon were characterized by high methane flux and high *u** (Figure 1.13). These diurnal trends in methane flux were significantly correlated with diurnal cycles of soil temperature in June and August (Table 1.4), and diurnal cycles in incoming shortwave radiation in July, August and September (Table 1.4). Diurnal variation in methane flux in July was also compared to diurnal variation in incoming short-wave radiation and ecosystem conductance (Table 1.5). Ecosystem conductance was calculated from eddy-covariance measurements of latent heat flux, relative humidity and atmospheric pressure. Both variation in short-wave radiation and ecosystem conductance were significantly correlated with variation in methane flux, however, short-wave radiation had a stronger relationship.

To further investigate diurnal trends in methane flux, the difference between average daytime and nighttime methane flux was compared. Daytime was defined as any period where PPFD was greater than 50 μmol m^{-2} s^{-1}. Data were then grouped by daytime or nighttime and by month to test for differences in daytime and nighttime methane flux and monthly patterns in methane flux. A significant difference between daytime and nighttime methane flux was found, as well as a significant monthly

pattern in the NEE of methane, under every *u** screening (Table 1.6). A significant difference between daytime and nighttime methane flux was evident in monthly data plots, where in every month except May, under every *u** screening, daytime methane flux values exceeded nighttime methane flux values (Figure 1.14). Significant monthly variation in methane flux was also apparent, where average daytime and nighttime methane flux increased until a peak in July, with a gradual decrease in average methane flux from July through September, under every *u** screening (Figure 1.14).

In order to explain seasonal variation in methane flux, I evaluated the effect of changes in known environmental controls on methane flux. A strong exponential relationship between daily average methane flux and daily average soil temperature was found, where a soil temperature increase, resulted in an associated increase in methane flux (Figure 1.15). Based on the exponential relationship between soil temperature and methane flux, and the relationship between water table depth and methane flux, I was able to predict seasonal variation in daily average methane flux, using equation 2:

$$NEE\ CH_4(nmol\ m^{-2}s^{-1}) = 19.495 \bullet 7.255^{\frac{(Ts-10)}{10}} \qquad (3)$$

where NEE CH_4 was the daily average net ecosystem exchange of CH_4, 19.495 was the estimated value of net methane flux capacity at 10 ºC, 7.255 was the estimated Q_{10} value or the change in net methane flux per 10 ºC increase in temperature and Ts

was the daily average soil temperature. Predicted daily average methane flux and measured daily average methane flux corresponded well with an $R^2 = 0.646$. Additional functions describing atmospheric pressure, GPP and multiple combinations of each were tested for accuracy in predicting methane flux. The use of these functions did not significantly improve predictions of methane flux, with the best predictions of methane NEE being based on soil temperature (Table 1.7). Soil temperature-based predictions of daily average methane flux corresponded well with measured daily average methane flux throughout the growing season (Figure 1.16). Data points that deviated strongly from the predicted seasonal pattern were usually average data points calculated from only a few reliable measurements on that day (eg. where greater than 80 % of daily data was missing). Due to the good correspondence between predicted and measured daily average methane data, equation 2 was used to predict daily average methane flux in order to gap-fill missing methane flux measurements.

Gap-filled methane flux data allowed the calculation of a monthly-integrated methane flux (Figure 1.17). July had the highest integrated methane efflux, with May having the lowest. However, the May value was calculated from only 10 days of data and, therefore, did not adequately represent the entire month. September and June both displayed low but comparable methane flux values. The largest increase in integrated methane efflux occurred from June to July, displaying an increase of over 80 mmol m^{-2} $month^{-1}$. After this large increase, integrated CH_4 efflux gradually decreased for the remainder of the growing season.

In addition to evaluating the environmental controls of methane flux, seasonal variation the capacity for methane emission at 10 ºC (R_{10}) was also considered. The R_{10} values were estimated by non-linear regression analysis:

$$NEE\ CH_4 = R_{10} \bullet Q_{10}^{(\frac{(Ts-10)}{10})} \quad (4)$$

where Q_{10} was the change in NEE, per 10 ºC increase in soil temperature. Q_{10} varied as a function of soil temperature to account for acclimation of soil microbes (i.e. Q_{10} = 3 - 0.045*Ts) (Tjoelker et al., 2001; Wythers et al., 2005), Ts was the soil temperature and NEE CH_4 was the net ecosystem exchange of methane for each half hour. R_{10} was calculated over a 10 day period using 30-minute data values of Ts and NEE CH_4. R_{10} showed seasonal variation with maximum capacity measured in late July, and minimum capacity measured in late May (Figure 1.18 a). This variation corresponded well with changes in soil temperature, where an increase in soil temperature correlated well with an increase in R_{10} (Figure 1.18 b). Seasonal variation in R_{10} was also correlated with seasonal variation in GPP (Figure 1.18 c), although this relationship was not as strong as that observed between soil temperature and R_{10}.

1.3.3 Peatland global warming potential

There was seasonal variation in the daily-integrated GPP, with late June and early July displaying peak values (Figure 1.19). The peatland served as a net sink of CO_2 for all months in the growing season (May - September) (Figure 1.20), but served as a net source of CO_2 in all other months (October - April). Integrated over the 2007 growing season, a CO_2 influx of 18.5 mol m^{-2} was measured.

The reduction in radiative forcing due to CO_2 sequestration was offset by 34 % by emitted methane, under the 20year time horizon (Figure 1.21). Methane emission had less of an influence on radiative forcing when considered over longer time horizons. Under the 100-year and 500-year time horizons, the reduction in radiative forcing due to CO_2 sequestration was offset by 11 % and 4 % by methane emission, respectively (Figure 1.21).

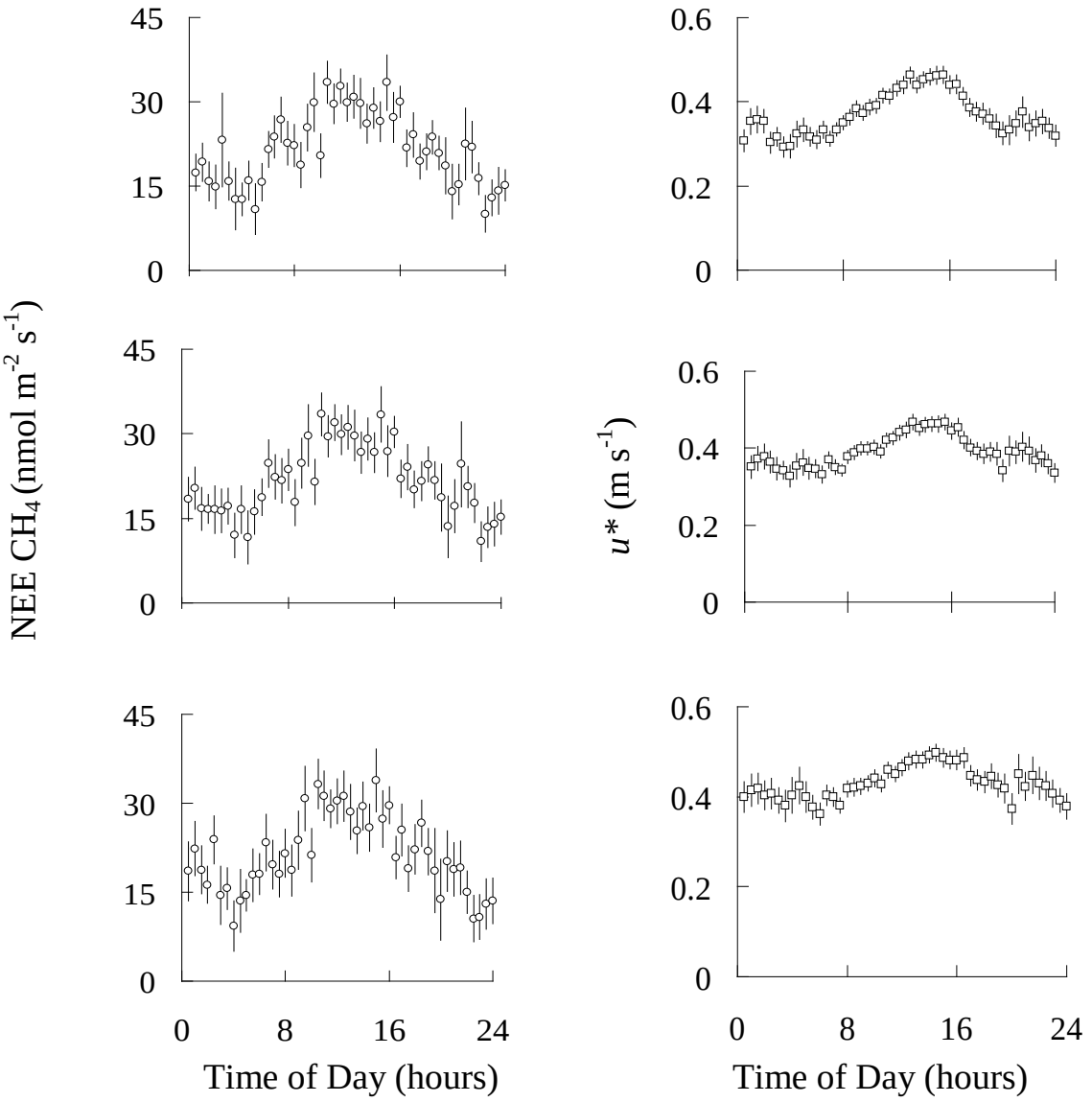

Figure 1.13: The average diurnal cycle of methane flux (left column) and u^* (right column) under a u^* threshold of 0.15 m s^{-1} (upper graph), 0.18 m s^{-1} (middle graph) and variable threshold based on month (lower graph). Each diurnal plot is a bin average data for a given time of day, over the entire growing season.

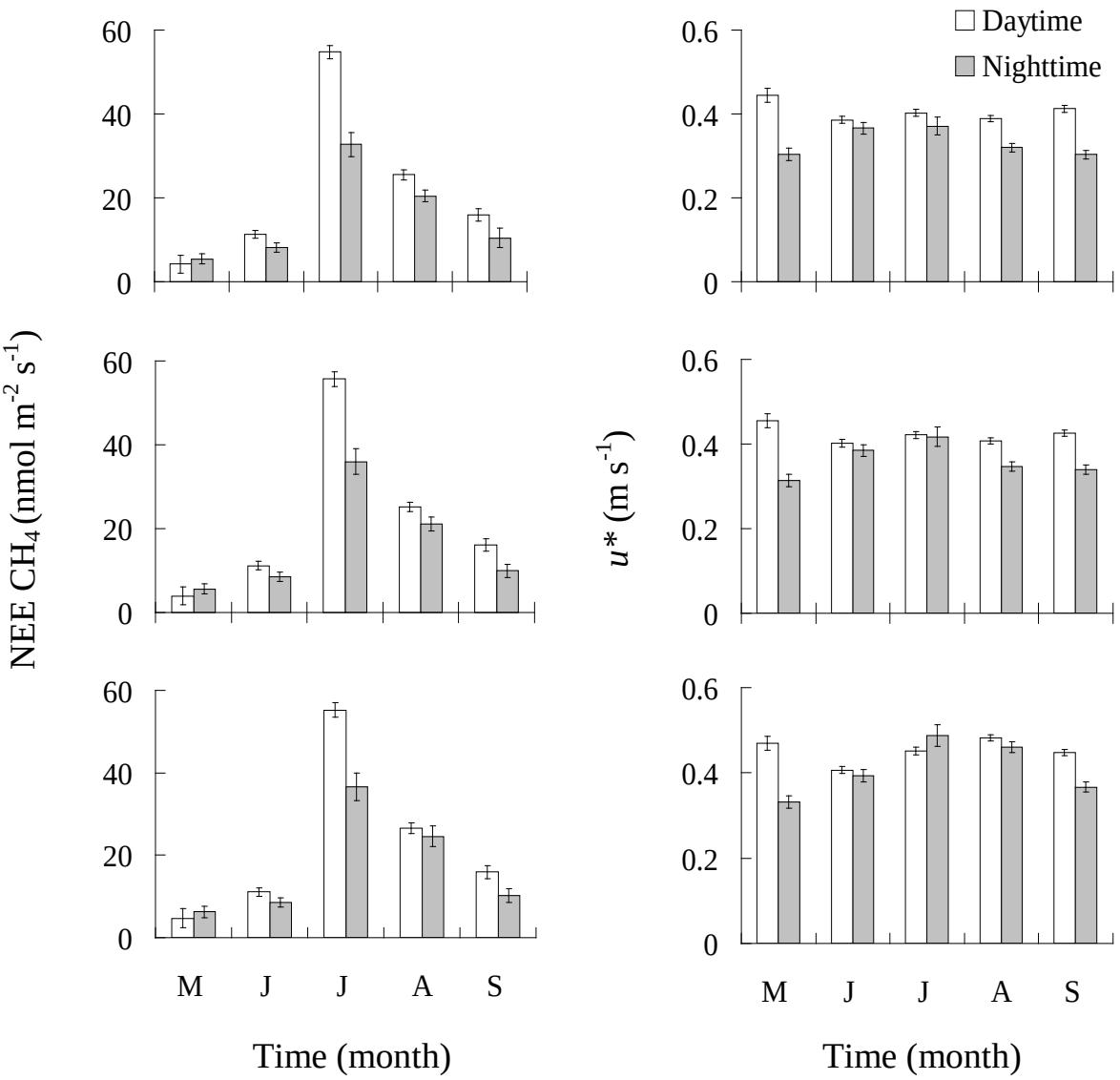

Figure 1.14: A comparison of daytime and nighttime variation in methane flux (left column) and friction velocity (u^*) (right column), with a u^* screening of $u^* > 0.15$ (upper graph), $u^* > 0.18$ (middle graph) and u^* variable monthly value (lower graph). Values represent the average methane flux ± SEM and average u^* ± SEM. All measurements were taken at the western peatland flux station, in northern Alberta.

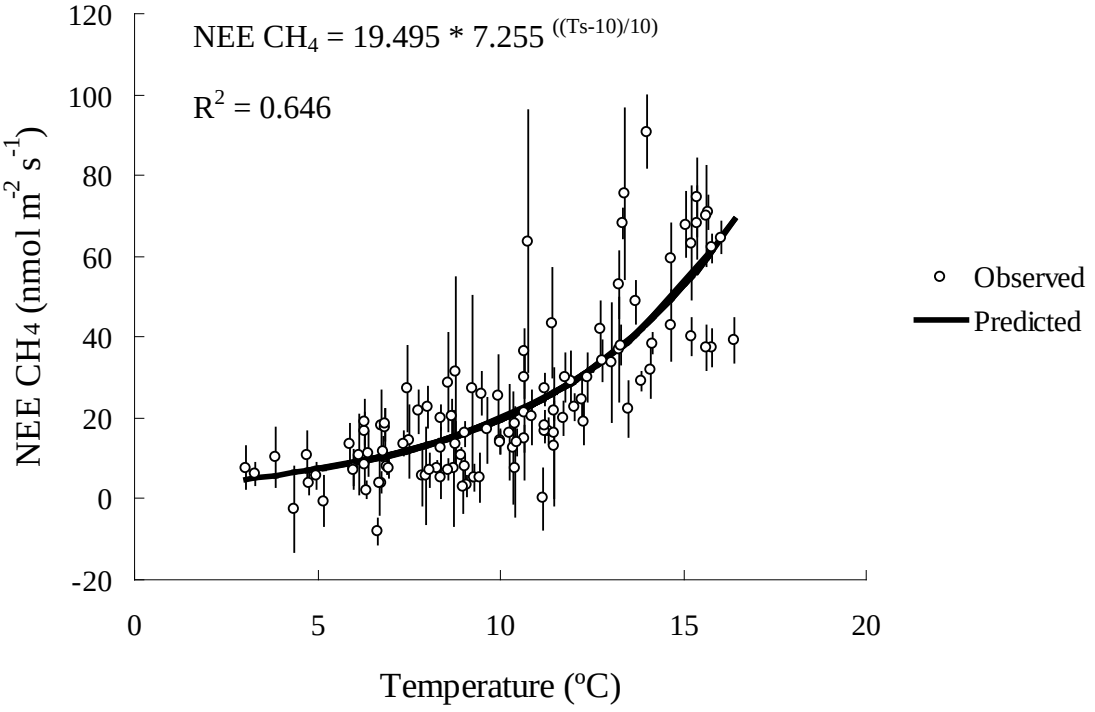

Figure 1.15: A comparison between daily averaged soil temperature and daily average NEE of CH_4 ± SEM. Predicted values of daily average NEE of CH_4 were calculated from daily average soil temperature within the zone of methane production.

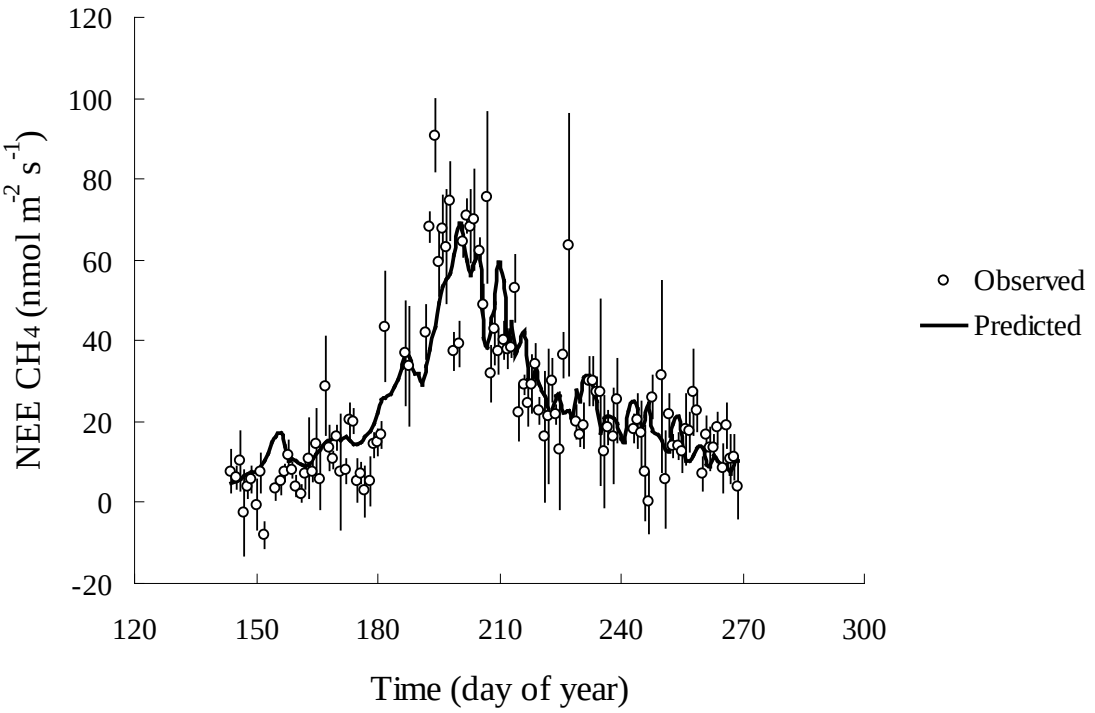

Figure 1.16: The daily average NEE of CH_4 ± SEM for May through September of the 2007 growing season. Predicted values are estimates of daily average methane flux calculated with equation 2, based on soil temperature.

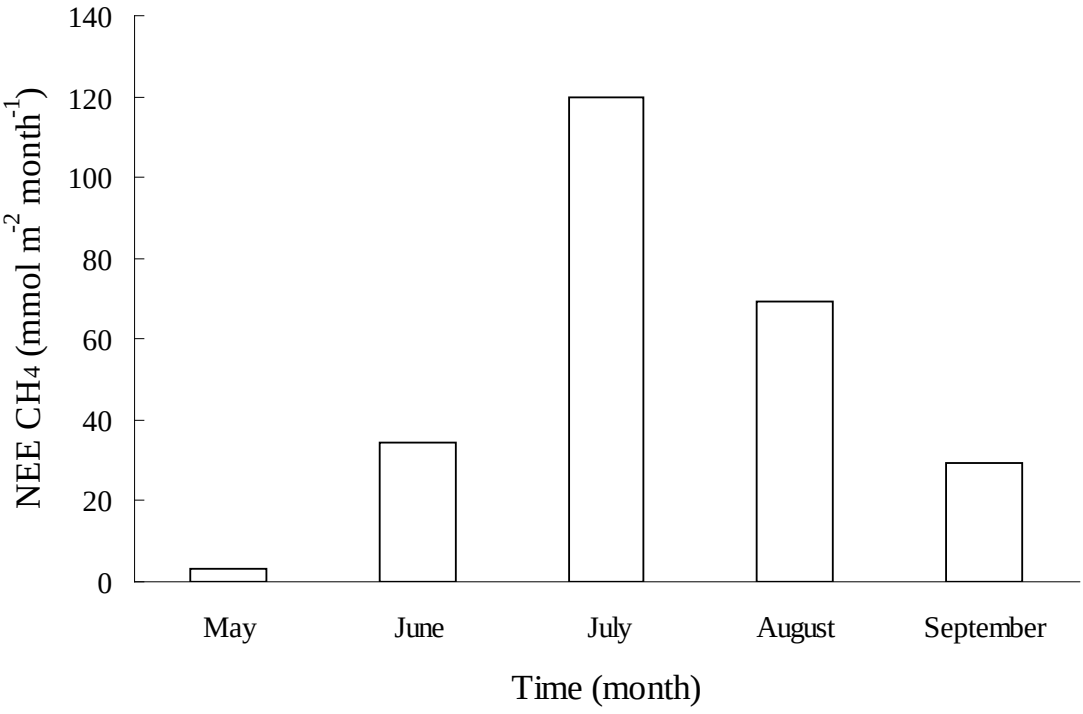

Figure 1.17: The monthly integrated methane flux for May – September of the 2007 growing season. All measurements were taken at the western peatland flux station, in northern Alberta.

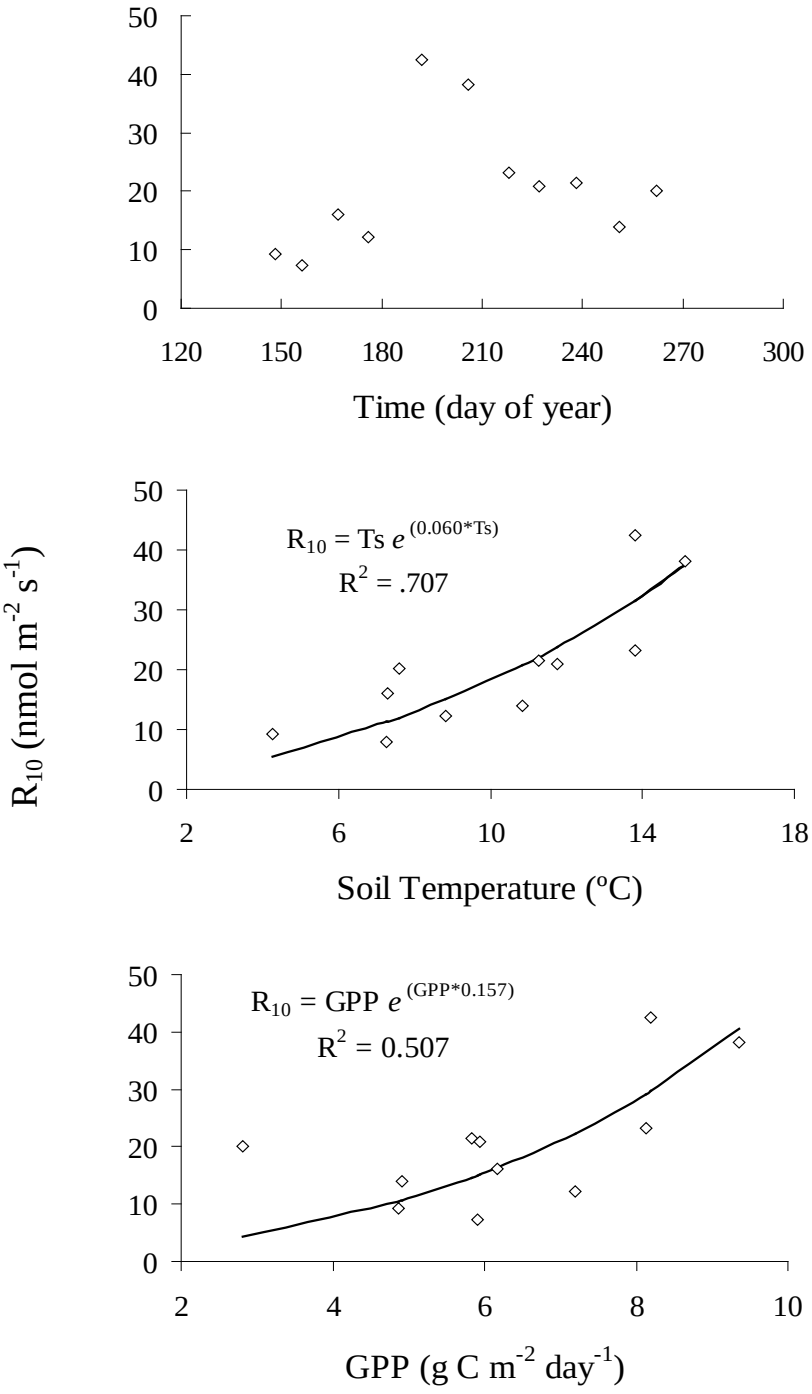

Figure 1.18: The estimated capacity for methane production at 10 ºC (R_{10}) throughout the growing season (upper graph), for a given soil temperature (middle graph) and at measured values of GPP (lower graph). Each data point represents a 10-day period throughout the growing season, with soil temperature and GPP averaged for each respective time period.

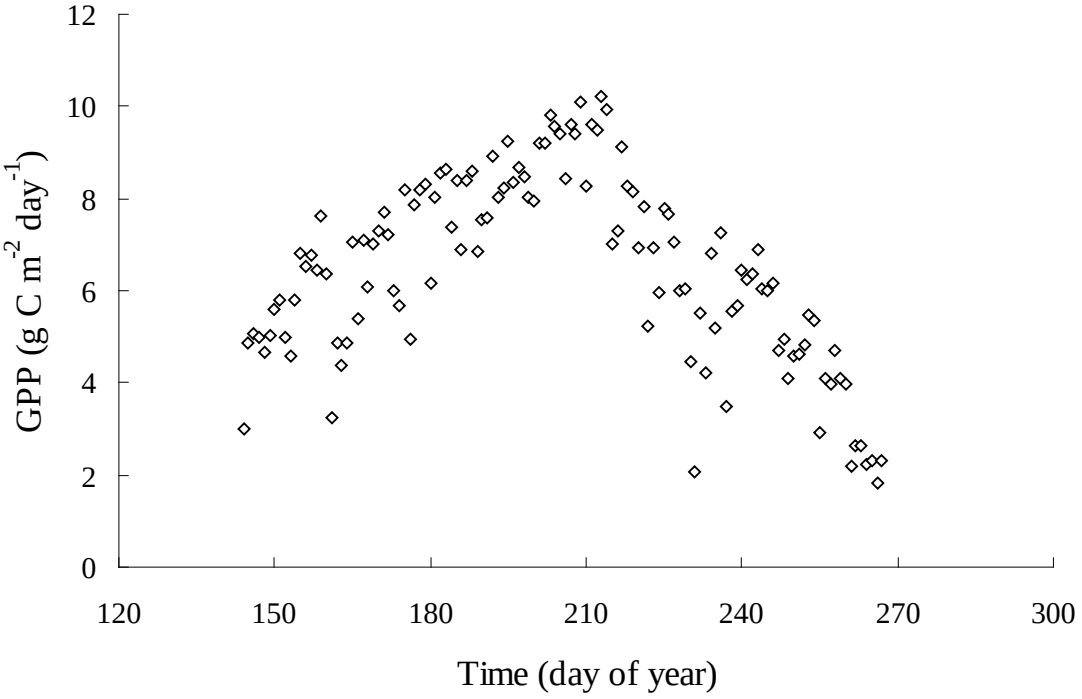

Figure 1.19: The daily integrated gross primary productivity (GPP) for the study site, throughout the 2007 growing season. Positive values denote uptake of CO_2 by the peatland.

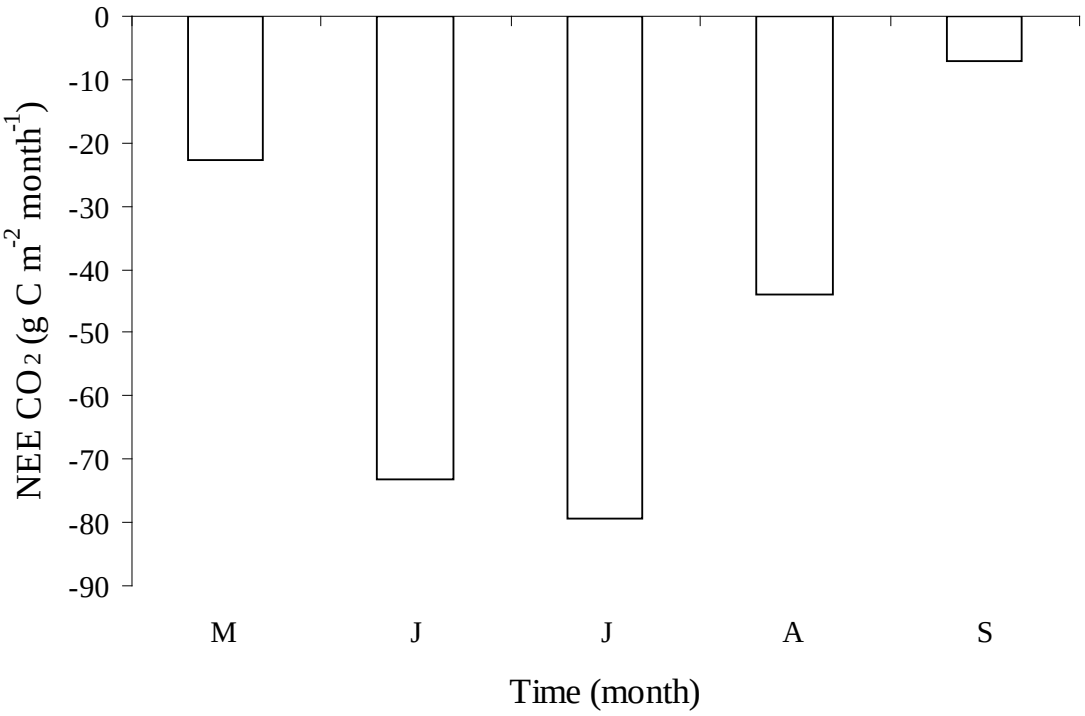

Figure 1.20: The monthly integrated net ecosystem CO_2 flux for the 2007 growing season. Negative values denote uptake of CO_2 by the peatland. All measurements were taken at the western peatland flux station, in northern Alberta.

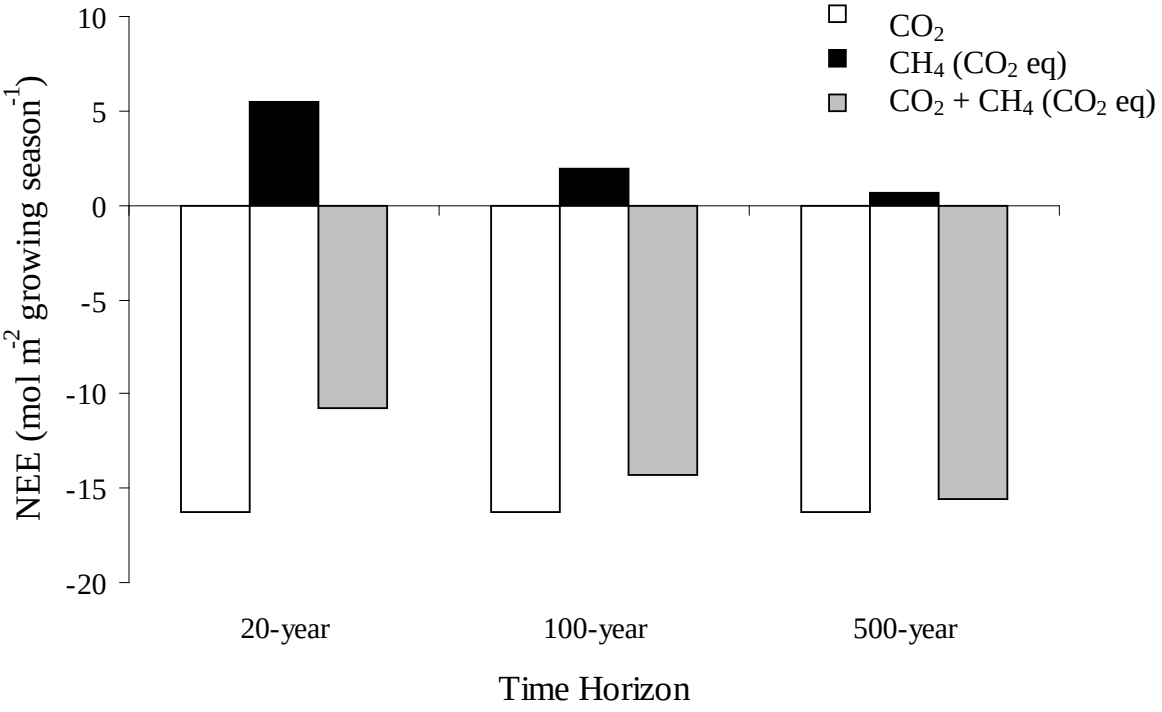

Figure 1.21. The 2007 growing season calculation of net ecosystem exchange (NEE) of CO_2, CH_4 in CO_2 equivalents (CH_4 (CO_2 eq)) and CO_2 equivalents (CO_2 + CH_4 (CO_2 eq)). Growing season results represent the integrated seasonal flux for May - September under the 20, 100 and 500-year time horizons.

Table 1.2. An analysis of variance (ANOVA) testing the significance of diurnal trends in methane flux, for the entire 2007 growing season, under three different *u** screening methods. Data was grouped by a half-hourly (30-minute) intervals, for a given time of day.

Screening	df	F-ratio	P
$u^* > 0.15$ m s^{-1}	47	2.27	< 0.001
error	2702		
$u^* > 0.18$ m s^{-1}	47	2.026	< 0.001
error	2464		
u^* > variable monthly screening	47	1.772	0.001
error	2044		

Table 1.3 An analysis of variance (ANOVA) testing the significance of diurnal trends in u^*, for the entire 2007 growing season, under three different u^* screening methods. Data was grouped by a half-hourly (30-minute) intervals, for a given time of day.

Screening	df	F-ratio	P
$u^* > 0.15$ m s^{-1}	47	5.5	< 0.001
error	2702		
$u^* > 0.18$ m s^{-1}	47	3.478	< 0.001
error	2464		
u^* > variable monthly screening	47	2.41	< 0.001
error	2044		

Table 1.4: The correlation of soil temperature and incoming short-wave radiation with diurnal cycles of net methane emission. Values were bin averaged by time of day, for each month of the growing season.

Month	Soil Temperature (correlation coefficient)	Radiation (correlation coefficient)
May	-0.101	-0.162
June	-0.323*	0.133
July	-0.156	0.757*
August	0.369*	0.386*
September	0.269	0.415*

* indicates correlation coefficients as significant ($p<0.05$)

Table 1.5: The correlation of incoming short-wave radiation (30-minute values) and ecosystem conductance (30-minute values) with net methane emission (30-minute values) in July. Ecosystem conductance calculations were based on measurements of latent heat flux, VPD and atmospheric pressure.

Variable	Radiation (correlation coefficient)	Conductance (correlation coefficient)
NEE CH_4	0.377*	0.244*

* indicates correlation coefficients as significant ($p<0.001$)

Table 1.6. An analysis of variance (ANOVA) testing the significance of day/night and monthly trends in methane flux, as well as the interaction between day/night and monthly trends in methane flux, for the 2007 growing season, under three different *u** screening methods. Data were grouped as day/night, where daytime was defined as any point in the day where PPFD > 50 µmol m^{-2} s^{-1} and night was defined as any point in the day where PPFD < 50 µmol m^{-2} s^{-1}. Monthly data was grouped as growing season month (i.e. May, June, July, August and September), when methane flux data was collected.

Screening	df	F-ratio	P
*u** > 0.15 m s^{-1}			
Day/Night	1	24.146	< 0.001
Month	4	101.521	< 0.001
Interaction term	4	8.119	< 0.001
error	2740		
*u** > 0.18 m s^{-1}			
Day/Night	1	19.187	< 0.001
Month	4	107.036	< 0.001
Interaction term	4	6.152	< 0.001
error	2502		
*u** > variable monthly screening			
Day/Night	1	12.376	< 0.001
Month	4	88.258	< 0.001
Interaction term	4	4.636	0.001
error	2082		

Table 1.7: A non-linear regression analysis where models were fit to daily average methane flux. NEE = net ecosystem exchange of methane (nmol m^{-2} s^{-1}), $Ts = a * b^{((\text{soil temperature}-10)/10)}$, WT = c*(water table position + 200)/200 (where 200 cm equals the average peat depth), S = 10-day average GPP, used as a proxy for methanogenic substrate concentration and $P = d^{(Pobs- Pref)}$ (where Pobs is the observed atmospheric pressure and Pref is the average atmospheric pressure within the data set).

Data fitting model	R^2
NEE = Ts	0.646
NEE = Ts * WT	0.649
NEE = Ts * S	0.627
NEE = Ts * P	0.646
NEE = Ts * WT * S	0.633
NEE = Ts * WT * P	0.649
NEE = Ts * WT * S * P	0.634

1.4 Discussion

1.4.1 Influence of friction velocity on methane flux

Two different friction velocity (u^*) thresholds were characterized, the seasonal ($u^* > 0.18$ m s^{-1}) and monthly variable threshold values. A u^* threshold value was selected as the point where an increase in turbulence no longer significantly increased methane flux. In setting these u^* thresholds, any influence of turbulence on the observed methane fluxes may have been removed. Removing this effect from the analyses could be problematic because turbulence has been proposed as a possible environmental driver of methane flux (Wille et al., 2008) and in one instance was indicated as the most important factor controlling ecosystem-scale methane flux (Sachs et al., 2008).

Wille et al. (2008) and Sachs et al. (2008) both showed exponential relationships between u^* and methane flux. Such an exponential relationship was not present within my data set. In contrast, a threshold u^* was identified where further increases in u^* no longer significantly increased methane flux. These differing relationships between u^* and methane flux may be due to the methods used in summarizing the data. Wille et al. (2008) summarized the relationship between u^* and methane flux by plotting daily average friction velocity and daily average methane flux. There was not a relationship between daily average u^* and daily average methane flux for the western peatland. The absence of a clear relationship was attributed to a high degree of seasonal variation in methane flux, coupled with a relatively constant daily average

*u** throughout the growing season. To resolve a possible confounding influence of seasonal variation in turbulence and methane flux, data was categorized by *u**, not by day of year. When this was done, an increase in methane flux with an increase in friction velocity was observed at low *u** values, whereas at higher *u** values, an increase in friction velocity did not significantly increase methane flux (entire growing season, Figure 1.3; within each individual month, Figure 1.4). My results may also have differed from Wille et al. (2008) because of variation in study site characteristics. The study site used by Wille et al. (2008) and Sachs et al. (2008) had large areas of open water, where turbulence would have a substantial effect on methane emission (Fan et al., 1992). At the site used within this study, there were no significantly sized areas of open water and so turbulence was not expected to have the same influence on methane flux.

Wille et al. (2008) were able to successfully model methane flux for an entire growing season with an exponential function describing the relationship between turbulence and methane flux. However, in an analysis of the same study site in 2006, Sachs et al. (2008) found the model proposed by Wille et al. (2008) overestimated methane flux at high values of methane NEE. Sachs et al. (2008) were successful in resolving overestimations of methane flux by adding an additional function to the model describing an influence of atmospheric pressure on methane flux. However, overestimation of methane flux may have been due to the fact that Wille et al (2008) used an exponential relationship, where it was not warranted. In the Sachs et al (2008) study, days of high turbulence corresponded with days of high methane flux,

therefore, the Wille et al. (2008) model may have overestimated 2006 fluxes due to the turbulence function predicting increased methane flux with increased u^*, when turbulence no longer had an influence on methane flux. If turbulence was no longer having an influence on methane flux at high u^* values (as is indicated in my data set), the Wille et al. (2008) and Sachs et al. (2008) model could be improved by revising their relationship between turbulence and methane flux.

1.4.2 Controls on diurnal cycles in methane flux

Significant diurnal variation in methane flux was found over the entire growing season, under every u^* screening (Table 1.2; Figure 1.13). Data suggested that turbulence was not a major control of diurnal cycles of methane flux. This was supported by a significant correlation between every seasonal diurnal cycle in methane flux. If turbulence was a major contributor to diurnal cycles in methane flux, a difference would be observed between a u^* threshold of 0.15 m s^{-1}, which included a small influence of turbulence on methane flux and the other u^* thresholds. However, differences between u^* screenings were not observed, which indicated that turbulence was not an important control of methane flux within this analysis. The lack of difference between the analysis that included an influence of turbulence and other u^* thresholds was due to only 10 % of data being influenced by turbulence with a u^* threshold of 0.15 m s^{-1}, where was under other thresholds turbulence was not influencing net methane emission. This was not a large enough proportion of the data set to significantly change the pattern in diurnal cycles in methane flux from one screening to another. Due to only 10 % of data points being influenced by turbulence

after screening, turbulence was not indicated as an important control of diurnal variation in methane flux at this study site.

To better understand the relationship between diurnal cycles in methane flux and friction velocity, differences between daytime and nighttime values of each measurement were compared. Daytime values of net methane emission and friction velocity were significantly higher than nighttime values (Table 1.4), over the entire growing season, under every u^* screening. However, changes in friction velocity within each individual month could not explain differences in methane flux. There were months within the analysis where daytime and nighttime values of friction velocity were not significantly different, whereas daytime methane flux was always higher than nighttime flux (Figure 1.14). In addition, during July under the monthly variable u^* threshold, mean nighttime friction velocity exceeded the daytime value, but mean daytime methane flux was higher than nighttime methane flux. These results suggest that there are other important controls on methane flux that cause high daytime fluxes and low nighttime fluxes.

Diurnal cycles in methane flux have previously been attributed to diurnal fluctuations in i) soil temperature (Alford et al., 1997; Seiler et al., 1984; Zhu et al., 2007), ii) convective flow through wetland plants (Chanton et al., 1993; Whiting and Chanton, 1996) and iii) stomatal conductance (Garnet et al., 2005; Hirota et al., 2004; Morrissey et al., 1993). Diurnal cycles in temperature are thought to control methane flux due to increased soil temperatures during the day, resulting in increased methane

flux during the day. There was a diurnal cycle in soil temperature over the entire growing season (Figure 1.9), however, when considering each month individually, soil temperature was only significantly correlated with the diurnal cycle in methane flux in June and August (Table 1.4). However, within June the correlation coefficient was negative, indicating that an increase in temperature resulted in a decrease in net methane emission. To further investigate diurnal cycles in temperature relation to diurnal cycles in methane flux, temperature was categorized by daytime and nighttime for each month. In May and July, there were no significant differences between daytime and nighttime soil temperature and in June nighttime soil temperature was higher than daytime. With no significant differences in daytime and nighttime soil temperatures in July and nighttime temperatures higher than daytime temperature in June, variation in soil temperature could not explain the difference between daytime and nighttime methane fluxes within these months. This indicates that there were other factors within June and July, other than temperature, which contributed to diurnal variation in methane flux. In August and September, daytime soil temperature was higher than nighttime soil temperature (Figure 1.10), therefore, soil temperature may have contributed to differences in daytime and nighttime methane fluxes within these months. Since changes in soil temperature could not fully explain diurnal fluctuations in methane flux, other possible explanations were sought for the observed diurnal cycle.

Diurnal cycles in methane flux can be influenced by above ground vegetation acting as a conduit for methane from the anaerobic root zone to the atmosphere. Gases will

move through wetland plants by two processes, molecular diffusion (Barber et al., 1962; Koncalova et al., 1988; Lee et al., 1981; Moog and Bruggemann, 1998) and convective flow (Armstrong, 1979; Chanton et al., 1993; Dacey, 1981a; Dacey, 1981b; Whiting and Chanton, 1996). Molecular diffusion transports molecules down a concentration gradient, where high concentrations of oxygen within leaves diffuse to rooting zones where oxygen is scarce. This is enhanced by aerenchyma (Sachs, 1882), a specialized plant tissue that acts as a conduit for oxygen to move from the atmosphere to flooded root systems (Armstrong, 1978; Armstrong, 1979; Dacey, 1981a; Dacey, 1981b). Similar to the process for oxygen (but opposite in direction), methane that has diffused into the root system will diffuse through plant stem aerenchyma and out to the atmosphere. Convective flow is a process where gas moves throughout wetland plants by increased pressure created within young leaves and stems, forcing gases into the root zone. As gas is forced into the root system by increased pressure in young leaves, gases within the rooting system are vented out through old leaves and stems (Dacey, 1981b). Increased pressure within young leaves can be caused by two factors, increased temperature (Dacey, 1981a; Dacey, 1981b) and differences in relative humidity between the inner leaf and atmosphere (Armstrong and Armstrong, 1991). With high pressure created within young leaves, oxygen and other atmospheric gases are forced into the lower root system and in doing so methane will be forced out of the lower roots and vented to the atmosphere through old leaves and stems.

Diurnal changes in methane flux can result from aquatic plants undergoing a switch from diffusive gas transport at night, to the more efficient (i.e. faster) convective flow during the day (Whiting and Chanton, 1996). Diurnal changes in methane flux can also be influenced by stomatal conductance, where methane diffusion through aerenchymous tissue is restricted or permitted as stomata close an open. The influence of stomatal conductance has been debated (Chanton et al., 1993; Whiting and Chanton, 1996), although multiple studies have shown the influence of stomatal opening and closure on methane flux (Frye et al., 1994; Garnet et al., 2005; Hirota et al., 2004; Morrissey et al., 1993).

In order to determine whether convective flow or stomatal conductance controlled methane flux, methane flux was correlated with ecosystem conductance (a proxy for stomatal opening) and shortwave radiation (a proxy for convective flow) within July. Shortwave radiation was used as a proxy for convective flow because it will determine leaf temperature, a major control on convective flow. Also, July was the only month considered within this analysis because it had the largest magnitude of diurnal change in methane flux and because daytime soil temperature was not significantly different from nighttime soil temperature (Figure 1.14). A stronger correlation was found between incoming shortwave radiation and methane flux (Table 1.5), suggesting that convective flow was influencing methane flux more so than stomatal conductance (Table 1.5), however both convective flow and stomatal conductance may have both influenced net methane emission.

Evidence was presented suggesting that diurnal variation in temperature and pressurized bulk flow were possible contributors to diurnal variation in methane flux. Although evidence was presented suggesting differing controls on methane flux, it is likely that combinations of factors contributed to methane flux.

1.4.3 Seasonal variation in methane flux

Seasonal variation in daily average methane flux was strongly correlated with soil temperature (Figure 1.15). My observation of an increase in methane flux resulting from an increase in soil temperature was consistent with several previous studies describing soil temperature as a strong control of methane flux (Crill et al., 1988; Macdonald et al., 1998; Williams and Crawford, 1984). In addition, previous studies have shown an exponential relationship between soil temperature and methane flux (Elberling et al., 2008; Hargreaves et al., 2001; Wille et al., 2008), which was consistent with my findings. Although a strong relationship between soil temperature and methane flux was found, a Q_{10} value (7.255) was calculated that was greater than several previously determined Q_{10} values in minerotrophic peat (Q_{10} = 1.5 - 6.4) (Segers, 1998; Valentine et al., 1994; Westermann and Ahring, 1987; Williams and Crawford, 1984). The high Q_{10} was the result of multiple factors. When predicting daily average methane flux, I did not take into consideration methanogenic substrate availability. GPP has been used as a proxy for methanogenic substrate availability, where periods of high methane production coincided with periods of high GPP (Whiting and Chanton, 1993). As GPP increases, more substrate is available for methane production, therefore, an increase in GPP results in methane production

which can result in an increase in net methane emission. Within my data set, periods of peak methane production (Figure 1.16) coincided with periods of peak GPP (Figure 1.19). By not initially considering this relationship within equation 2, an artificially high temperature response coefficient was calculated. Had substrate availability been taken into account, a lower Q_{10} would have been calculated.

In the initial analysis seasonal changes in the capacity for methane emission at 10 ºC (R_{10}) were not taken into account. In order to fit equation 2 to measured daily average methane flux, a high Q_{10} was needed to compensate for lack of seasonal variation in R_{10}. Subsequent analyses completed showed that seasonal variation in R_{10} was an important control on methane flux. This is significant because changes in respiration capacity have not normally been taken into consideration when predicting fluxes from peatlands. By not including this relationship, the influence of other environmental factors on methane flux may be misinterpreted. The increase in R_{10} throughout the growing season was closely correlated to an increase in soil temperature (Figure 1.18 a), indicating soil temperature as an important contributor to seasonal variation in R_{10}. Also seasonal variation in R_{10} was correlated with GPP (Figure 1.18 c), although this relationship was not as strong as the relationship between R_{10} and soil temperature. This indicated that soil temperature change had more of an influence on changes in R_{10} than GPP. The increase in R_{10} associated with changes in soil temperature and GPP was likely the result of an increase in microbial biomass. As more resources become available for methane production (i.e. increased GPP) and conditions are more conducive to metabolic activity (i.e. increased soil temperature),

the environment can sustain larger populations of methanogenic microorganisms. If the microbial biomass increased (as suggested by R_{10}), so too will the environment's capacity to produce methane, which was observed within this analysis. This analysis has highlighted the need to consider changes in R_{10} when interpreting information about the controls on methane flux.

Seasonal variation in methane flux did not correlate well with changes in water table depth (Figure 1.12) or turbulence (data not shown) (Table 1.7). The lack of evidence suggesting that water table depth was an important control on methane flux was consistent with Rinne et al. (2007), where water table position was not considered a controlling factor of methane flux. However, this was not consistent with other studies that found a correlation between methane flux and water table position (McNamara et al., 2006; Moore and Roulet, 1993; Roulet et al., 1993), indicating water table position as a control of methane flux. Lack of evidence suggesting water table depth as a strong control on methane flux may have been due to changes of R_{10}, temperature and GPP affecting methane flux more so than changes in water table.

The strong correlation between methane flux and soil temperature allowed soil temperature measurements to be used for predicting methane flux at times when observations were missing. Such a gap-filling technique allowed calculations of daily and monthly-integrated methane flux. For my study site, a total integrated methane efflux of 0.26 mol m^{-2} (4.1 g CH_4 m^{-2}) was calculated for May - September 2007. This value was low compared to values reported in most other studies of methane flux

from fen ecosystems (Heikkinen et al., 2002; Koch et al., 2007; Rask et al., 2002; Rinne et al., 2007; Suyker et al., 1996) but comparable to rates reported in two studies (Roulet et al., 1992; Saarnio et al., 2007). Northern peatlands have shown a range in average net methane emission from 3 mg m^{-2} day^{-1} (Roulet et al., 1992) to 181 mg m^{-2} day^{-1} (Suyker et al., 1996). My study site had an average net methane emission of 32 mg m^{-2} day^{-1}. The low rate of methane flux was most likely due to a low water table when compared to other studies (Koch et al., 2007; Rask et al., 2002). Although variation in water table depth was not found to be a strong control on seasonal variation in methane flux in this study, a consistently low water table throughout the growing season (Figure 1.12) would limit net methane emission in two ways. First, it would decrease the anaerobic soil volume for methane production. With a smaller soil volume for production, methane efflux should decrease. Second, a low water table increases the zone of methane oxidation. As the zone of methane oxidation increases, more methane is oxidized, which results in a reduced net methane emission. The combination of a reduced zone of methane production, coupled with an increased zone of methane oxidation was most likely responsible for the low methane flux observed in this study.

Using the values of seasonal integrated methane efflux, the net greenhouse budget for the peatland was calculated. In order to determine the net greenhouse gas budget of the peatland a comparison between methane emission and CO_2 sequestration was made. When present within the atmosphere, methane will contribute more to radiative forcing than CO_2 on a per mole basis. Therefore, in order to compare methane flux

with CO_2 flux, methane was converted to CO_2 equivalents. In addition, time horizons of 20, 100 and 500-years were considered in my analysis. A time horizon refers to the amount of time that sequestered carbon remains resident within soil. As the time horizon increases, the contribution of methane to radiative forcing relative to CO_2 is lessened. The peatland acted as a net sink of greenhouse gases for the 2007 growing season, under every time horizon evaluated (Figure 1.21). Under a 20-year time horizon, greater than 34 % of CO_2 sequestration was offset by methane emission. This is not a substantial offset in comparison with other studies (Corradi et al., 2005; Friborg et al., 2003; Hendriks et al., 2007; Whiting and Chanton, 2001). In evaluating the radiative forcing budget of a peatland ecosystem characterized by slow decomposition, a longer time horizon is more representative of carbon soil residence time. Therefore, in assessing my study site's greenhouse gas balance, a 500-year time horizon is more likely representative of the radiative forcing relationship between methane and CO_2 flux. Under a 500-year time horizon, the influence of methane on the greenhouse gas balance was small, offsetting CO_2 sequestration by less than 5 %. The greenhouse carbon balance under the 500-year time horizon indicated that the peatland was acting as a substantial sink of greenhouse gases, for the 2007 growing season.

Using a constant time horizon to compare CO_2 sequestration with CH_4 emission was suggested to inaccurately describe the relationship between CO_2 and CH_4 flux from peatlands (Frolking et al., 2006). Frolking et al. (2006) considered peatlands as an infinite sink of CO_2, continually removing CO_2 from the atmosphere, and storing it as

organic matter within soil. A continual net CO_2 sink would result in a continual reduction in radiative forcing, with an increase in time. Methane dynamics differ from CO_2, because there is a relatively short atmospheric turnover time of methane (~11 years (IPCC, 2001)). All methane emitted to the atmosphere will be removed after approximately 11 years. A constant rate of methane removal coupled with a constant rate of methane emission will result in an equilibrium concentration within the atmosphere. This will result in methane having a constant radiative forcing within the atmosphere, as time increases. Due to emitted methane achieving radiative forcing equilibrium and CO_2 sequestration continually removing radiative forcing agents from the atmosphere, there is a point where radiative forcing caused by methane emission equals the reduction in radiative forcing caused by CO_2 sequestration. This point is referred to as the switchover time, and is dependent on the ratio of methane emission to CO_2 sequestration. Once a switchover time is achieved, the peatland is acting as a net sink of greenhouse gases. If the ratio of methane emission to CO_2 sequestration is less than 0.012 mol mol^{-1}, the radiative forcing reduction due to CO_2 sequestration is greater than radiative forcing caused by methane emission. Within this study, the ratio of methane emission to CO_2 sequestration was 0.015 mol mol^{-1}, therefore the study site would only be contributing to radiative forcing for a short period of time, until it began serving as a net sink of greenhouse gases.

Two possible important components of an ecosystem's greenhouse carbon budget have been excluded from this analysis, dissolved carbon loss and non-methane volatile organic compound (NMVOCs) efflux. Dissolved carbon loss is where

organic carbon, inorganic carbon and methane are dissolved within water and will exit the ecosystem as runoff. This will reduce the magnitude of sink when considering the total carbon budget of an ecosystem by reducing carbon accumulation. Past studies have shown dissolved carbon exiting the ecosystem to offset carbon accumulation minimally (3 % of NEE CO_2 offset by dissolved carbon loss) (Rivers et al., 1998), moderately (31 % - 41 % of NEE CO_2 offset by dissolved carbon loss) (Nilsson et al., 2008; Roulet et al., 2007) and substantially (100 % of NEE CO_2 offset by dissolved carbon loss) (Billett et al., 2004). NMVOCs are greenhouse gases and will influence an ecosystem's greenhouse gas balance by vegetation emitting NMVOCs to the atmosphere throughout the growing season. In a study by Bäckstrand et al. (2008), it has been reported that NMVOCs can significantly contribute to the radiative balance of an ecosystem. I did not take measurements of dissolved carbon loss and NMVOCs for the 2007 growing season; therefore I can not assess their contribution to the carbon balance for my study site. In future work, dissolved carbon loss and NMVOCs should be considered to gain a full understanding of the greenhouse carbon budget of an ecosystem.

1.5 Conclusions

A significant diurnal trend in net methane emission was found for the 2007 growing season. Methane flux was correlated with diurnal variation in soil temperature within some months of the growing season, but not others. Also, diurnal variation in methane flux was correlated with diurnal variation in incoming short-wave radiation. These results suggested that diurnal variation in methane flux was due to changes in

soil temperature within some months and changes in incoming short-wave radiation in other months, or a combination of both effects.

I have shown a strong seasonal variation in methane flux, which was attributed to seasonal variation in the capacity for methane emission, soil temperature and GPP. Results suggest that the major mechanism was a change in soil temperature causing a change in the capacity for methane emission. This resulted in an increase in net methane efflux.

The correlation between soil temperature and daily average methane flux was used as a gap-filling tool, to fill missing methane flux data points. Gap filled data allowed the calculation of a monthly and season long integrated methane flux to be compared integrated CO_2 flux. In comparing methane and CO_2 flux, I found that the peatland was acting as a substantial sink of radiative forcing agents, for the entire growing season.

2 Aerobic methanogenesis in actively growing *Sphagnum* mosses

2.1 Introduction

The concentration of atmospheric methane has risen drastically since the pre-industrial times. However, recently atmospheric concentrations of methane have appeared to level off and are no longer increasing (IPCC, 2001). The cause of the leveling off of atmospheric methane concentrations is not yet resolved, but it has recently been proposed that the cease in atmospheric methane concentration increase is due to the deforestation of tropical rainforests (Keppler et al., 2006). This hypothesis stems from a highly controversial paper by Keppler et al. (2006) that proposed aerobic methane production by plants, which would explain previous observations of high methane concentrations found above tropical rainforests (Dlugokencky et al., 2003; Dlugokencky et al., 1998; do Carmo et al., 2006). Keppler et al. (2006) faced criticism following publication based on perceived weaknesses in their experimental methods and scaling up approaches (Kirschbaum et al., 2006).

In a follow up paper, Dueck et al. (2007) found no evidence for aerobic methane production by plants that were used within the Keppler et al. (2006) analysis, in particular *Zea mays* L., which had the highest methane emission of any plant tested by Keppler et al. (2006). Aerobic methane emission from *Zea mays* L. was also tested by Beerling et al. (2008), where again, no evidence was found supporting aerobic methane production by plants. Although Dueck et al. (2007) and Beerling et al. (2008) were not able to find any evidence of methane emission by plants, other

results have been published supporting the hypothesis that some plants can produce methane aerobically. Sanhueza and Donoso (2006) found evidence of methane production from savanna grasses by comparing plots of actively growing grass with plots where grass was clipped. The plots containing actively growing grass showed higher methane emission than the clipped plots, though problems persist with the Sanhueza and Donoso (2006) analysis. Peak methane emission was observed following rain events which may have created anaerobic microsites in the soil which were capable of methane production. Furthermore, the difference in methane emission between clipped and unclipped plots can be accounted for by a reduction in methanogenic substrate, which would occur by removing above ground vegetation. Wang et al. (2008) also found evidence of aerobic methane emission from plants growing on the inner Mongolia Steppe. Though specific plant species were found to produce methane aerobically, the majority of species tested did not emit methane. In a paper by Vigano et al. (2008), aerobic methane emission from plants occurred when plant material was exposed to UVB light. Vigano et al. (2008) were able to find emission of the methane from a high proportion of plant species tested. This study was important because it proposed a possible explanation for the Dueck et al. (2007) and Beerling et al. (2008) studies finding little evidence supporting aerobic methane production by plants. Both Dueck et al. (2007) and Beerling et al. (2008) applied photosynthetically active light (PAR) (400 nm - 700 nm), but did not apply light with any UVB wavelengths (280 nm - 315 nm). In addition to providing an explanation for the negative results of Dueck et al. (2007) and Beerling et al. (2008), Vigano et al. (2008) tested plant litter from the Dueck et al. (2007) study, and found evidence for

aerobic methane emission. Though Vigano et al. (2008) and Wang et al. (2008) both tested several plant species for aerobic methane emission, *Sphagnum* moss has yet to be examined, a predominant plant type within boreal wetlands.

It was the objective of this study to test if *Sphagnum* moss could produce methane aerobically. *Sphagnum* moss was selected because it was the predominant moss genus at the study site where season long eddy covariance measurements of net methane flux were conducted.

2.2 Methods

2.2.1 Moss samples

Moss samples were collected at the western peatland flux station of the Canadian Carbon Program (formerly Fluxnet Canada), in August of 2007. For a complete study site description, see Chapter 1. Moss samples were collected by cutting out 60 x 30 x 20 cm *Sphagnum* spp. lawn and placing the lawn within large plastic containers. The moss lawns extracted were uniform in colour and moss species present. Within 24 hours of moss extraction, samples were transported to the University of Lethbridge, where they were placed within modified PVC collars in tubs of 1.5 % modified Hoagland's solution. PVC collars were equipped with a wire mesh to suspend moss samples within the modified Hoagland's solution. Samples were grown at room temperature (approximately 20 ^{o}C), under coolwhite fluorescent lighting, which provided approximately 120 µmol m^{-2} s^{-1} of photosynthetic photon flux density

(PPFD), for 14 hours per day. The moss samples remained under these growing conditions for 4 months until trials began in January, 2008.

2.2.2 Flux measurements

Moss samples were placed within an inverted water jacket glass chamber equipped with a mixing fan (Micronel ® US, Vista, California, USA), UVB light source (Exo-Terra, USA), copper-constantan thermocouples and gallium arsenide photosynthetically active radiation (PAR) sensor (Appendix 1 - Water jacketed chamber). The fan was used to ensure adequate mixing of air in the chamber, thermocouples measured moss and air temperature and the gallium arsenide PPFD sensor was used to assess PPFD throughout the experiment. All components within the chamber were suspended from a clear PVC plastic plate. The PVC plate was then placed over the open end of an inverted water jacketed chamber to seal the chamber from outside air. High vacuum grease (Dow Corning Corporation, Midland, Michigan) was used to seal the connection between the PVC plastic plate and the chamber. The UVB light source, thermocouples and PPFD sensor pass through locations of the PVC plate were all sealed with qubitac sealant (Qubit Systems Inc, Kingston, Ontario, Canada). In order to control chamber temperature, temperature regulated water was cycled though the water jacketed chamber by a water bath (VWR Scientific Products, West Chester, Pennsylvania, USA).

A light spectrum was conducted on the UVB light source via spectroradiometer (Analytical Spectral Devices, Boulder, Colorado, USA). A complete UVB spectrum was not able to be conducted due to the spectroradiometer only reading to a minimum

of 350 nm. In order to account for UVB radiation, spectral values were inferred between 280 - 349 nm based on manufacturer's specifications of UV radiation. The total incoming radiation for UVB, UVA and PAR produced by the light source was calculated (Figure 2.1). Photosynthetically active radiation (PAR) was measured from the UVB light for every sample. The UVB light provided PAR at a constant rate of 170 µmol m^{-2} s^{-1} for every treatment.

Once the chamber was sealed with moss samples within, it was then "charged" with air from a supply tank. The tank supplied the chamber and tubing with air until the chamber equilibrated to the desired treatment temperature (approximately 30 minutes). The system was then closed off from the supply tank, and air within the chamber was cycled throughout the tubing and chamber system by an LI-6262 reference pump (LICOR, Lincoln, Nebraska, USA) for 90 minutes. Air cycled throughout the chamber and tubing network was also passed though a LI-6262 CO_2/H_2O analyzer (LICOR, Lincoln, Nebraska, USA) in order to measure CO_2 and H_2O vapour concentration. After the complete 90 minute cycle, a 40 cc sample was drawn from a septum located on the system tubing. The sample was then injected into a septum connected to a tunable diode laser absorption spectrometer (TDLAS) TGA100A (Campbell Scientific, Logan, Utah, USA) to measure methane concentration (Appendix 2 - Closed chamber aerobic CH4 flux measurement).

To inject the sample into the TGA100A, the sample line was equipped with a septum, mass-flow controller (MKS instruments, Andover, Massachusetts, USA) and a carrier

gas with a methane concentration of approximately 7 ppb (Praxair, Edmonton, Alberta, Canada). The septum served as the sample injection location, the mass-flow controller served to regulate the rate at which the carrier gas entered the sample line and the carrier gas was used in order to transport the sample from the injection septum, to the TGA100A. In order measure an injection of 40 cc, a low flow rate into the TGA100A was needed to measure methane concentration. The carrier gas flow rate was set at 60 mL min^{-1} for every sample injected. In order to dry air samples, a PD-IT nafion sample dryer was installed (Campbell Scientific, Logan, Utah, USA) between the injection septum and the TGA100A. This dryer was capable of drying the low gas flow (< 200 mL/min) used in the study.

In order to test the precision of measuring methane concentration of injected samples, a precision test was conducted (Table 2.1). The injection of tank air displayed high precision with a range of 20 ppb for all injections with a standard deviation of 10 ppb. A measurement of flux required accuracy in measuring the difference between two gases. In order to evaluate the TGA100A accuracy in measuring difference between two gases, calibrations were performed with two high precision gases of known methane concentration. The known difference in calibration gas methane concentration was compared to measured difference in calibration gas methane concentration. Calibrations on the TGA100A returned an average difference of 115.2 ± 9.5 ppb (n = 5) between calibration gases, in comparison to an actual difference of 109.6 ppb.

In order to calculate the flux from the moss sample, the methane concentration within the sample which was drawn at the completion of the 90 minute gas cycling period, was compared to the methane concentration within the tank gas used to charge the chamber system. To measure the concentration of methane within the tank used to charge the system, a flask equipped with a septum was filled with tank gas. The gas within the flask was then drawn and injected into the TGA100 in the same manner as was the sample gas taken from the chamber system, immediately following the injection of the sample gas. An immediate injection is necessary in order to combat drift which is commonly associated with the TGA100A (Billesbach et al., 1988; Pattey et al., 2006). In order to measure CO_2 start and ending concentrations, chamber gas was cycled through a LI-6262 CO_2/H_2O analyzer, and a manual reading of CO_2 concentration was conducted at the beginning and end of each 90 minute sample cycle.

TGA100A data were collected with the TGA100A real time screen data collection control, which saved data files directly to the C-drive of the computer operating the TGA100. These files were then imported into Microsoft Office Excel (Microsoft Corporation, Bellevue, Washington, USA), for data analysis. All other data (i.e. PAR, moss temperature, air temperature) was collected by a CR23X data logger (Campbell Scientific, Logan, Utah, USA).

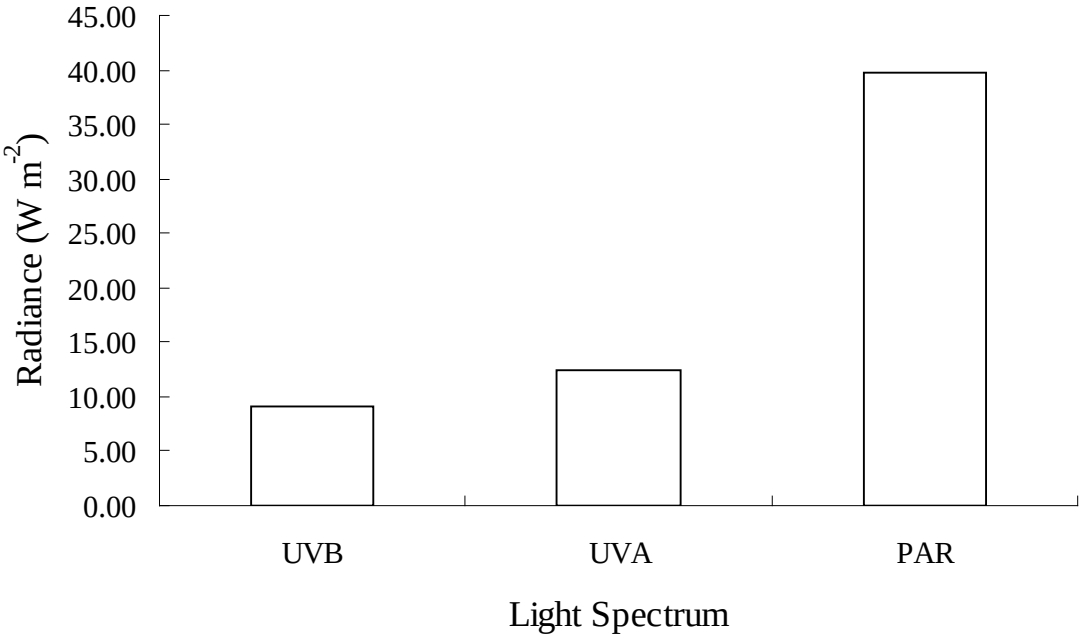

Figure 2.1: The total UVB, UVA and PAR produced by the light source provided to the *Sphagnum* spp. moss samples during methane flux measurements.

Table 2.1. A precision test of 4 samples injected into the TGA100 through a septum. All samples were taken from a sampling flask filled by the same tank gas. The tank gas had a concentration of 2100 ppb, measured previously by continuously flowing tank air through the TGA100A.

Sample	Measurement (ppb)	Mean	SD
1	2263	2248.25	9.91
2	2245		
3	2242		
4	2243		

2.2.3 Flux calculations

With the difference in methane and CO_2 concentrations known, gas flux was calculated as

$$flux\ (\mu g\ m^{-2}\ hr^{-1}) = \left(\frac{\Delta\,[gas] \bullet n}{a \bullet \Delta t} \right) \bullet 16 \qquad (5)$$

Where: Δ [gas] = change in methane concentration (µmol mol^{-1})
n = moles of air within the sample system (mol)
a = area of the moss sample (m^2)
t = time (hr)
16 = coefficient to convert flux to µg m^{-2} s^{-1} from µmol m^{-2} s^{-1}

Where the moles of air within the sampling system (n) were represented as

$$n = \frac{PV}{RT}$$

Where: P = atmospheric pressure (bar)
V = sample system volume (L)
R = universal gas constant (0.08314 L bar mol^{-1} K^{-1})
T = absolute temperature (K)

2.3 Results

Moss samples were acting as a net sink of methane, indicating a rate of methane production lower than the rate of methane consumption, at every temperature evaluated (Figure 2.2). In addition to observing a net uptake of methane into moss samples, a relationship was observed between methane flux and temperature, with an increase in temperature resulting in a reduction in methane uptake (Figure 2.2). The greatest methane uptake occurred at lower temperature with methane uptake decreasing as temperature increased. At 40 ºC, the samples were nearly neutral, having nearly no net methane flux. The mean methane flux values of the different temperature treatments were significantly different, indicating a significant influence of temperature on methane flux (Table 2.2).

Methane and CO_2 flux responded differently to increases in temperature. The increase in temperature resulted in a linear decrease of methane uptake, where as an increase in temperature resulted in a non-linear decrease of CO_2 uptake (Figure 2.2). There was little change in CO_2 assimilation between the 29 and 34 ºC, where as a significant difference was observed in methane flux (Figure 2.2). In addition, a large reduction in CO_2 assimilation was observed between the 34 and 41ºC temperature treatments; whereas the change in methane flux remained at a similar rate as observed between the 29 and 34 ºC treatments (Figure 2.2).

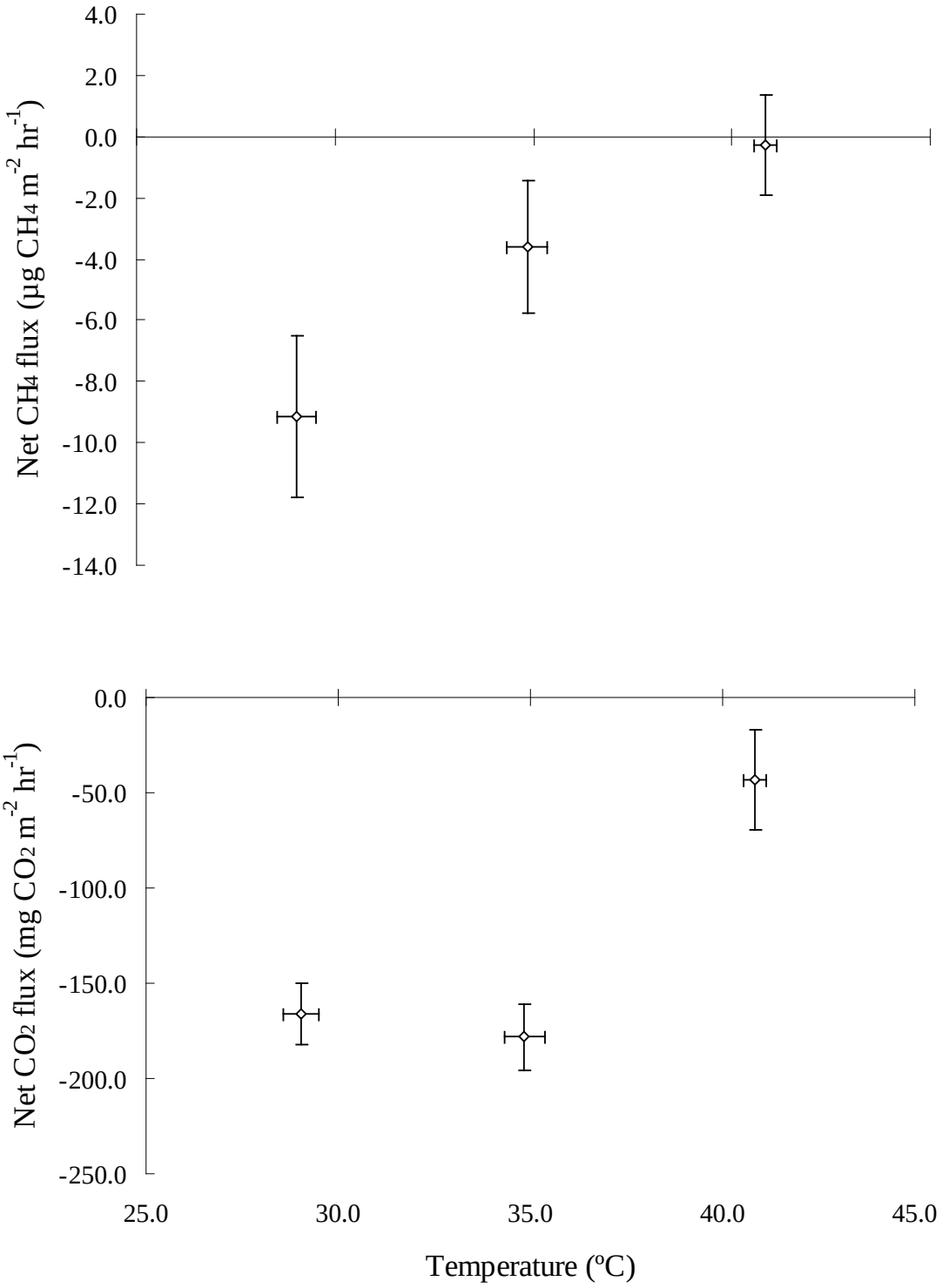

Figure 2.2: The influence of temperature ± SEM on average net methane flux ± SEM (upper graph) and average net CO_2 flux ± SEM (lower graph) of *Sphagnum* spp. moss samples. Flux values are presented as the sample - control.

Table 2.2: An analysis of variance (ANOVA) conducted on methane flux by *Sphagnum* spp. moss samples, under three temperature treatments.

Treatments (º C)	Mean ($\mu g\ m^{-2}\ s^{-1}$)	SE ($\mu g\ m^{-2}\ s^{-1}$)	n	P
30 ºC	-9.15	2.65	5	0.04
35 ºC	-3.62	2.16	5	
40 ºC	-0.27	1.51	5	

2.4 Discussion

No evidence was found in this study for aerobic methane production by *Sphagnum* spp. mosses. Furthermore, moss samples acted as a net sink of methane at all temperatures tested (Figure 2.2). These findings were not consistent with previous studies which showed aerobic methane production by various plant species (Keppler et al., 2006; Sanhueza and Donoso, 2006; Wang et al., 2008), but consistent with Dueck et al. (2007) and Beerling et al. (2008), studies that found no evidence for aerobic methane production by plants. Vigano et al. (2008) concluded that UVB radiation promoted the production of methane, and with some species, UVB radiation was needed to observe any methane emission. Within our experiment, moss species were exposed to UVB light (Figure 2.1), with no evidence of aerobic methane emission.

Sphagnum moss acting as a net sink of CH_4 under aerobic conditions is consistent with conventional knowledge of peatland methane fluxes. Peatland methane flux is controlled by methane production, which occurs within the flooded anaerobic zone, and methane oxidation, which occurs within the upper aerobic zone (Le Mer and Roger, 2001; Segers, 1998; Valentine et al., 1994; Zhuang et al., 2004). Microbes within the zone of methane oxidation (methanotrophs) will consume methane being produced by microbes within the zone of methane production (methanogens) (Holzapfelpschorn et al., 1986; Schutz et al., 1989). Also, methanotrophs can oxidize atmospheric methane resulting in a net influx for methane (Holmes et al., 1999; Kiese et al., 2008; Ridgwell et al., 1999). If methane influx exceeds methane efflux, the

peatland would be serving as a net sink of methane. This scenario occurs in upland forest and grassland areas, but is not common in peatlands due to high rates of methane production within the anaerobic soil zone. In the absence of an anaerobic environment, it would be likely to see a net influx of methane, as was observed within this experiment. These results indicate that any methane being produced aerobically by moss samples was less than methane consumption by methanotrophic organisms. A net uptake of methane, for every temperature treatment, indicated that aerobic methane production by *Sphagnum* spp. mosses was negligible and not of concern in estimated CH_4 fluxes from peatlands.

There was a significant relationship between methane uptake and temperature, with increasing temperature, resulting in a decrease in methane uptake (Table 2.2). This may have been caused by either a) an increase in aerobic methane production by moss samples, b) a decrease in methane oxidation, or a combination of both. With this experimental design, it was indeterminable if an increase in temperature caused an increase in aerobic methane production or a decrease in methane oxidation or both.

The mechanism responsible for aerobic methane production by plants is not yet understood, however, net methane and CO_2 flux reacted differently to increased temperature (Figure 2.2), indicating a different process influencing each. CO_2 flux will be governed primarily by photosynthetic and respiratory processes, where as methane flux will be controlled by methanotrophic microbial populations and/or aerobic methane production by the moss sample. If observed changes in methane flux

were due to aerobic methane production by moss, methane production is most likely exclusive from photosynthetic processes, as indicated by a different response of each process to an increase in temperature. No relationship between aerobic plant methane production and photosynthetic processes is consistent with previous studies that have hypothesized that plant derived methane originated from pectin (Keppler et al., 2006; Keppler et al., 2008). Pectin is a plant compound that serves no role in photosynthesis, therefore a relationship between photosynthesis and aerobic plant methane production was not expected.

2.5 Conclusion

I did not find any evidence of aerobic methane production by *Sphagnum* moss. Furthermore, moss samples were acting as a net sink of methane, between 30 - 40 ºC. My findings are consistent with aerobic zones within the peat profile acting as a net sink of methane due to methanotrophic microorganisms. With lack of evidence for aerobic methane production by *Sphagnum* moss, it is unlikely that aerobic methane production from these mosses is an important contributor to methane efflux at the western peatland flux station.

3 References

Alford, D.P., Delaune, R.D. and Lindau, C.W., 1997. Methane flux from Mississippi River deltaic plain wetlands. Biogeochemistry, 37: 227-236.

Armstrong, J. and Armstrong, W., 1990. Light-enhanced convective throughflow increases oxygenation in rhizomes and rhizosphere of *Phragmites australis* (Cav.) Trin. ex Steud. New Phytologist, 114: 121 - 128.

Armstrong, J. and Armstrong, W., 1991. A convective through-flow of gases in *Phragmites australis* (Cav) Trin Ex Steud. Aquatic Botany, 39: 75-88.

Armstrong, W., 1978. Root aeration in wetland conditions. In: D. E. Hook and R. M. M. Crawford (Editors), Plant Life in Anaerobic Environments. Ann Arbor Science Publishers, Ann Arbor, Michigan, USA, pp. 269 - 297.

Armstrong, W. (Editor), 1979. Aeration in higher plants. Advances in Botanical Research. Academic Press, London, UK.

Aubinet, M., Grelle, A., Ibrom, A., Rannik, U., Moncrieff, J., Foken, T., Kowalski, A.S., Martin, P.H., Berbigier, P., Bernhofer, C., Clement, R., Elbers, J., Granier, A., Grunwald, T., Morgenstern, K., Pilegaard, K., Rebmann, C., Snijders, W., Valentini, R. and Vesala, T., 2000. Estimates of the annual net carbon and water exchange of forests: The EUROFLUX methodology. Advances in Ecological Research, 30: 113-175.

Baldocchi, D.D., Hicks, B.B. and Meyers, T.P., 1988. Measuring biosphere-atmosphere exchanges of biologically related gases with micrometeorological methods. Ecology, 69: 1331-1340.

Barber, D.A., Ebert, M. and Evans, N.T.S., 1962. Movement of ^{15}O through barley and rice plants. Journal of Experimental Botany, 13: 397-403.

Barker, H.A., 1936. On the biochemistry of the methane fermentation. Archives of Microbiology, 7: 404 - 419

Beerling, D.J., Gardiner, T., Leggett, G., McLeod, A. and Quick, W.P., 2008. Missing methane emissions from leaves of terrestrial plants. Global Change Biology, 14: 1821-1826.

Bellisario, L.M., Bubier, J.L., Moore, T.R. and Chanton, J.P., 1999. Controls on CH_4 emissions from a northern peatland. Global Biogeochemical Cycles, 13: 81-91.

Billesbach, D.P., Kim, J., Clement, R.J., Verma, S.B. and Ullman, F.G., 1988. An intercomparison of two tunable diode laser spectrometers used for eddy correlation measurements of methane flux in a prairie wetland. Journal of Atmospheric and Oceanic Technology, 15: 197-206.

Billett, M.F., Palmer, S.M., Hope, D., Deacon, C., Storeton-West, R., Hargreaves, K.J., Flechard, C. and Fowler, D., 2004. Linking land-atmosphere-stream carbon fluxes in a lowland peatland system. Global Biogeochemical Cycles, 18: doi: 10.1029/2003GB002058.

Chanton, J.P. and Dacey, J.W.H. (Editors), 1991. Effects of vegetation on methane flux, reservoirs and carbon isotopic composition. . Trace Gas Emissions from Plants. Academic Press, San Diego.

Chanton, J.P., Whiting, G.J., Happell, J.D. and Gerard, G., 1993. Contrasting rates and diurnal patterns of methane emission from emergent aquatic macrophytes. Aquatic Botany, 46: 111-128.

Christensen, T.R., Ekberg, A., Strom, L., Mastepanov, M., Panikov, N., Mats, O., Svensson, B.H., Nykanen, H., Martikainen, P.J. and Oskarsson, H., 2003. Factors controlling large scale variations in methane emissions from wetlands. Geophysical Research Letters, 30: doi: 10.1029/2002L016848.

Cicerone, R.J. and Oremland, R.S., 1988. Biogeochemical aspects of atmospheric methane. Global Biogeochemical Cycles, 2: 299-327.

Corradi, C., Kolle, O., Walter, K., Zimov, S.A. and Schulze, E.D., 2005. Carbon dioxide and methane exchange of a north-east Siberian tussock tundra. Global Change Biology, 11: 1910 - 1925.

Crill, P.M., Bartlett, D.S., Harris, R.C., Gorham, E., Verry, E.S., Sebacher, D.I., Madzar, L. and Sanner, W., 1988. Methane flux from Minnesota peatlands. Global Biogeochemical Cycles, 2: 371-384.

Dacey, J.W.H., 1981a. How aquatic plants ventilate. Oceanus, 24: 43-51.

Dacey, J.W.H., 1981b. Pressurized ventilation in the yellow water-lily. Ecology, 62: 1137-1147.

Dlugokencky, E.J., Houweling, S., Bruhwiler, L., Masarie, K.A., Lang, P.M., Miller, J.B. and Tans, P.P., 2003. Atmospheric methane levels off: Temporary pause or a new steady-state? Geophysical Research Letters, 30: doi: 10.1029/2003GL018126.

Dlugokencky, E.J., Masarie, K.A., Lang, P.M. and Tans, P.P., 1998. Continuing decline in the growth rate of the atmospheric methane burden. Nature, 393: 447-450.

do Carmo, J.B., Keller, M., Dias, J.D., de Camargo, P.B. and Crill, P., 2006. A source of methane from upland forests in the Brazilian Amazon. Geophysical Research Letters, 33: doi: 10.1029/2005GL025436.

Dueck, T.A., de Visser, R., Poorter, H., Persijn, S., Gorissen, A., de Visser, W., Schapendonk, A., Verhagen, J., Snel, J., Harren, F.J.M., Ngai, A.K.Y., Verstappen, F., Bouwmeester, H., Voesenek, L.A.C.J. and van der Werf, A., 2007. No evidence for substantial aerobic methane emission by terrestrial plants: a ^{13}C-labelling approach. New Phytologist, 175: 29-35.

Einola, J.K.M., Kettunen, R.H. and Rintala, J.A., 2007. Responses of methane oxidation to temperature and water content in cover soil of a boreal landfill. Soil Biology & Biochemistry, 39: 1156-1164.

Elberling, B., Nordstrom, C., Grondahl, L., Sogaard, H., Friborg, T., Christensen, T.R., Strom, L., Marchand, F. and Nijs, I., 2008. High-arctic soil CO_2 and CH_4 production controlled by temperature, water, freezing and snow. Advances in Ecological Research, 40: 441-472.

Fan, S.M., Wofsy, S.C., Bakwin, P.S., Jacob, D.J., Anderson, S.M., Kebabian, P.L., Mcmanus, J.B., Kolb, C.E. and Fitzjarrald, D.R., 1992. Micrometeorological measurements of CH_4 and CO_2 exchange between the atmosphere and sub-arctic tundra. Journal of Geophysical Research-Atmospheres, 97: 16627-16643.

Friborg, T., Soegaard, H., Christensen, T.R., Lloyd, C.R. and Panikov, N.S., 2003. Siberian wetlands: Where a sink is a source. Geophysical Research Letters, 30: doi: 10.1029/2003GL017797.

Frolking, S., Roulet, N. and Fuglestvedt, J., 2006. How northern peatlands influence the Earth's radiative budget: Sustained methane emission versus sustained carbon sequestration. Journal of Geophysical Research-Biogeosciences, 111: doi: 10.1029/2005JG000091.

Frye, J.P., Mills, A.L. and Odum, W.E., 1994. Methane flux in *Peltandra virginica* (Araceae) wetlands: Comparison of field data with a mathematical model. American Journal of Botany, 81: 407-413.

Garnet, K.N., Megonigal, J.P., Litchfield, C. and Taylor, G.E., 2005. Physiological control of leaf methane emission from wetland plants. Aquatic Botany, 81: 141-155.

Gore, A.J.P. (Editor), 1983. Ecosystems of the world 4B. Mire: swamp, bog, fen and moor. Regional studies. Elsevier Scientific Publishing Co. , Amsterdam, NE.

Gorham, E., 1991. Northern peatlands - role in the carbon-cycle and probable responses to climatic warming. Ecological Applications, 1: 182-195.

Hargreaves, K.J., Fowler, D., Pitcairn, C.E.R. and Aurela, M., 2001. Annual methane emission from Finnish mires estimated from eddy covariance campaign measurements. Theoretical and Applied Climatology, 70: 203-213.

Heikkinen, J.E.P., Maijanen, M., Aurela, M., Hargreaves, K.J. and Martikainen, P.J., 2002. Carbon dioxide and methane dynamics in a sub-Arctic peatland in northern Finland. Polar Research, 21: 49-62.

Hendriks, D.M.D., van Huissteden, J., Dolman, A.J., van der Molen, M.K. and 2007. The full greenhouse gas balance of an abandoned peat meadow. Biogeosciences, 4: 411 - 424.

Heyer, J. and Berger, U., 2000. Methane emission from the coastal area in the southern Baltic Sea. Estuarine Coastal and Shelf Science, 51: 13-30.

Hirota, M., Tang, Y.H., Hu, Q.W., Hirata, S., Kato, T., Mo, W.H., Cao, G.M. and Mariko, S., 2004. Methane emissions from different vegetation zones in a Qinghai-Tibetan Plateau wetland. Soil Biology & Biochemistry, 36: 737-748.

Holmes, A.J., Roslev, P., McDonald, I.R., Iversen, N., Henriksen, K. and Murrell, J.C., 1999. Characterization of methanotrophic bacterial populations in soils showing atmospheric methane uptake. Applied and Environmental Microbiology, 65: 3312-3318.

Holzapfelpschorn, A., Conrad, R. and Seiler, W., 1986. Effects of vegetation on the emission of methane from submerged paddy soil. Plant and Soil, 92: 223-233.

IPCC, 2001. Climate change 2001: the scientific basis: contribution of working group I to the third assessment report of the Intergovernmental Panel on Climate Change. In: J. T. Houghten et al. (Editors). Cambridge University Press.

Joabsson, A. and Christensen, T.R., 2001. Methane emissions from wetlands and their relationship with vascular plants: an Arctic example. Global Change Biology, 7: 919-932.

Keppler, F., Hamilton, J.T.G., Brass, M. and Rockmann, T., 2006. Methane emissions from terrestrial plants under aerobic conditions. Nature, 439: 187-191.

Keppler, F., Hamilton, J.T.G., McRoberts, W.C., Vigano, I., Brass, M. and Rockmann, T., 2008. Methoxyl groups of plant pectin as a precursor of

atmospheric methane: evidence from deuterium labeling studies. New Phytologist, 178: 808-814.

Kiese, R., Wochele, S. and Butterbach-Bahl, K., 2008. Site specific and regional estimates of methane uptake by tropical rainforest soils in eastern Australia. Plant and Soil, 309: 211-226.

Kirschbaum, M.U.F., Bruhn, D., Etheridge, D.M., Evans, J.R., Farquhar, G.D., Gifford, R.M., Paul, K.I. and Winters, A.J., 2006. A comment on the quantitative significance of aerobic methane release by plants. Functional Plant Biology, 33: 521-530.

Koch, O., Tscherko, D. and Kandeler, E., 2007. Seasonal and diurnal net methane emissions from organic soils of the Eastern Alps, Austria: Effects of soil temperature, water balance, and plant biomass. Arctic Antarctic and Alpine Research, 39: 438-448.

Koncalova, H., Pokorny, J. and Kvet, J., 1988. Root ventilation in *Carex gracilis* Curt - diffusion or mass-flow. Aquatic Botany, 30: 149-155.

Le Mer, J. and Roger, P., 2001. Production, oxidation, emission and consumption of methane by soils: A review. European Journal of Soil Biology, 37: 25-50.

Lee, K.K., Holst, R.W., Watanabe, I. and App, A., 1981. Gas-transport through rice. Soil Science and Plant Nutrition, 27: 151-158.

Macdonald, J.A., Fowler, D., Hargreaves, K.J., Skiba, U., Leith, I.D. and Murray, M.B., 1998. Methane emission rates from a northern wetland: Response to temperature, water table and transport. Atmospheric Environment, 32: 3219-3227.

MacIntyre, S.R., Wanninkhof, R. and Chanton, J.P. (Editors), 1995. Trace gas exchange across the air-water interface in freshwater and coastal marine environments. Biogenic Trace Gases: Measuring Emissions from Soil and Water. Blackwell Publishing, Malden, Massachusetts.

McNamara, N.P., Chamberlain, P.M., Piearce, T.G., Sleep, D., Black, H.I.J., Reay, D.S. and Ineson, P., 2006. Impact of water table depth on forest soil methane turnover in laboratory soil cores deduced from natural abundance and tracer ^{13}C stable isotope experiments. Isotopes in Environmental and Health Studies, 42: 379-390.

Moncrieff, J.B., Massheder, J.M., deBruin, H., Elbers, J., Friborg, T., Heusinkveld, B., Kabat, P., Scott, S., Soegaard, H. and Verhoef, A., 1997. A system to measure surface fluxes of momentum, sensible heat, water vapour and carbon dioxide. Journal of Hydrology, 189: 589-611.

Moog, P.R. and Bruggemann, W., 1998. Flooding tolerance of *Carex* species. II. Root gas-exchange capacity. Planta, 207: 199-206.

Moore, T.R. and Roulet, N.T., 1993. Methane flux - water-table relations in northern wetlands. Geophysical Research Letters, 20: 587-590.

Morrissey, L.A., Zobel, D.B. and Livingston, G.P., 1993. Significance of stomatal control on methane release from *Carex*-dominated wetlands. Chemosphere, 26: 339-355.

Nilsson, M., Sagerfors, J., Buffam, I., Laudon, H., Eriksson, T., Grelle, A., Klemedtssons, L., Wesliens, P. and Lindroth, A., 2008. Contemporary carbon accumulation in a boreal oligotrophic minerogenic mire - a significant sink and accounting for all C-fluxes. Global Change Biology, 14: 2317 - 2332.

Nouchi, I., Mariko, S. and Aoki, K., 1990. Mechanism of methane transport from the rhizosphere to the atmosphere through rice plants. Plant Physiology, 94: 59-66.

Pattey, E., Strachan, I.B., Desjardins, R.L., Edwards, G.C., Dow, D. and MacPherson, J.I., 2006. Application of a tunable diode laser to the measurement of CH_4 and N_2O fluxes from field to landscape scale using several micrometeorological techniques. Agricultural and Forest Meteorology, 136: 222-236.

Post, W.M., Emanuel, W.R., Zinke, P.J. and Stangenberger, A.G., 1982. Soil carbon pools and world life zones. Nature, 298: 156-159.

Rask, H., Schoenau, J. and Anderson, D., 2002. Factors influencing methane flux from a boreal forest wetland in Saskatchewan, Canada. Soil Biology & Biochemistry, 34: 435-443.

Ridgwell, A.J., Marshall, S.J. and Gregson, K., 1999. Consumption of atmospheric methane by soils: A process-based model. Global Biogeochemical Cycles, 13: 59-70.

Rinne, J., Riutta, T., Pihlatie, M., Aurela, M., Haapanala, S., Tuovinen, J.P., Tuittila, E.S. and Vesala, T., 2007. Annual cycle of methane emission from a boreal fen measured by the eddy covariance technique. Tellus Series B-Chemical and Physical Meteorology, 59: 449-457.

Rivers, J.S., Siegel, D.I., Chasar, L.S., Chanton, J.P., Glaser, P.H., Roulet, N.T. and McKenzie, J.M., 1998. A stochastic appraisal of the annual carbon budget of a large circumboreal peatland, Rapid River Watershed, northern Minnesota. Global Biogeochemical Cycles, 12: 715-727.

Roulet, N.T., Ash, R. and Moore, T.R., 1992. Low boreal wetlands as a source of atmospheric methane. Journal of Geophysical Research-Atmospheres, 97: 3739-3749.

Roulet, N.T., Ash, R., Quinton, W. and Moore, T., 1993. Methane flux from drained northern peatlands - Effect of a persistent water-table lowering on flux. Global Biogeochemical Cycles, 7: 749-769.

Roulet, N.T., Lafleur, P.M., Richard, P.J.H., Moore, T.R., Humphreys, E.R. and Bubier, J., 2007. Contemporary carbon balance and late Holocene carbon accumulation in a northern peatland. Global Change Biology, 13: 397-411.

Saarnio, S., Morero, M., Shurpali, N.J., Tuittila, E.S., Makila, M. and Alm, J., 2007. Annual CO_2 and CH_4 fluxes of pristine boreal mires as a background for the lifecycle analyses of peat energy. Boreal Environment Research, 12: 101-113.

Sachs, J.A. (Editor), 1882. A text book of botany. Oxford University Press, Oxford, UK.

Sachs, T., Wille, C., Boike, J. and Kutzbach, L., 2008. Environmental controls on ecosystem-scale CH_4 emission from polygonal tundra in the Lena River Delta, Siberia. Journal of Geophysical Research-Biogeosciences, 113: doi: 10.1029/2007JG000505.

Sanhueza, E. and Donoso, L., 2006. Methane emission from tropical savanna *Trachypogon* sp. grasses. Atmospheric Chemistry and Physics, 6: 5315-5319.

Schlesinger, W.H. (Editor), 1997. Biogeochemistry: An analysis of global change. Academic Press, San Diego, California.

Schutz, H., Seiler, W. and Conrad, R., 1989. Processes involved in formation and emission of methane in rice paddies. Biogeochemistry, 7: 33-53.

Sebacher, D.I., Harriss, R.C. and Bartlett, K.B., 1985. Methane emissions to the atmosphere through aquatic plants. Journal of Environmental Quality, 14: 40-46.

Segers, R., 1998. Methane production and methane consumption: a review of processes underlying wetland methane fluxes. Biogeochemistry, 41: 23-51.

Seiler, W., Holzapfelpschorn, A., Conrad, R. and Scharffe, D., 1984. Methane emission from rice paddies. Journal of Atmospheric Chemistry, 1: 241-268.

Shine, K.P. and Forster, P.M.D., 1999. The effect of human activity on radiative forcing of climate change: a review of recent developments. Global and Planetary Change, 20: 205-225.

Strom, L., Ekberg, A., Mastepanov, M. and Christensen, T.R., 2003. The effect of vascular plants on carbon turnover and methane emissions from a tundra wetland. Global Change Biology, 9: 1185-1192.

Suyker, A.E., Verma, S.B., Clement, R.J. and Billesbach, D.P., 1996. Methane flux in a boreal fen: Season-long measurement by eddy correlation. Journal of Geophysical Research-Atmospheres, 101: 28637 - 28647.

Syed, K.H., Flanagan, L.B., Carlson, P.J., Glenn, A.J. and Van Gaalen, K.E., 2006. Environmental control of net ecosystem CO_2 exchange in a treed, moderately rich fen in northern Alberta. Agricultural and Forest Meteorology, 140: 97-114.

Tjoelker, M.G., Oleksyn, J. and Reich, P.B., 2001. Modelling respiration of vegetation: evidence for a general temperature-dependent Q_{10}. Global Change Biology, 7: 223-230.

Valentine, D.W., Holland, E.A. and Schimel, D.S., 1994. Ecosystem and physiological controls over methane production in northern wetlands. Journal of Geophysical Research-Atmospheres, 99: 1563-1571.

Verma, S.B., Ullman, F.G., Billesbach, D., Clement, R.J., Kim, J. and Verry, E.S., 1992. Eddy-correlation measurements of methane flux in a northern peatland ecosystem. Boundary-Layer Meteorology, 58: 289-304.

Vigano, I., van Weelden, H., Holzinger, R., Keppler, F., McLeod, A. and Rockmann, T., 2008. Effect of UV radiation and temperature on the emission of methane from plant biomass and structural components. Biogeosciences, 5: 937-947.

Visvanathan, C., Pokhrel, D., Cheimchaisri, W., Hettiaratchi, J.P.A. and Wu, J.S., 1999. Methanotrophic activities in tropical landfill cover soils: effects of temperature, moisture content and methane concentration. Waste Management & Research, 17: 313-323.

Vitt, D.H., Halsey, L.A., Thorman, M.N. and Martin, T., 1998. Peatland inventory of Alberta. Phase 1: Overview of peatland resources in the natural regions and subregions of the province, University of Alberta, Edmonton, AB.

Wang, Z.P. and Han, X.G., 2005. Diurnal variation in methane emissions in relation to plants and environmental variables in the Inner Mongolia marshes. Atmospheric Environment, 39: 6295-6305.

Wang, Z.P., Han, X.G., Wang, G.G., Song, Y. and Gulledge, J., 2008. Aerobic methane emission from plants in the inner Mongolia steppe. Environmental Science & Technology, 42: 62-68.

Wanninkhof, R. and McGillis, W.R., 1999. A cubic relationship between air-sea CO_2 exchange and wind speed. Geophysical Research Letters, 26: 1889-1892.

Westermann, P. and Ahring, B.K., 1987. Dynamics of methane production, sulfate reduction, and denitrification in a permanently waterlogged alder swamp. Applied and Environmental Microbiology, 53: 2554-2559.

Whiting, G.J. and Chanton, J.P., 1993. Primary production control of methane emission from wetlands. Nature, 364: 794-795.

Whiting, G.J. and Chanton, J.P., 1996. Control of the diurnal pattern of methane emission from emergent aquatic macrophytes by gas transport mechanisms. Aquatic Botany, 54: 237-253.

Whiting, G.J. and Chanton, J.P., 2001. Greenhouse carbon balance of wetlands: methane emission versus carbon sequestration. Tellus Series B-Chemical and Physical Meteorology, 53: 521-528.

Wille, C., Kutzbach, L., Sachs, T., Wagner, D. and Pfeiffer, E.M., 2008. Methane emission from Siberian arctic polygonal tundra: eddy covariance measurements and modeling. Global Change Biology, 14: 1395-1408.

Williams, R.T. and Crawford, R.L., 1984. Methane production in Minnesota peatlands. Applied and Environmental Microbiology, 47: 1266-1271.

Wolfe, R.S., 1971. Microbial formation of methane. Advances in Microbial Physiology, 6: 107 -146.

Wythers, K.R., Reich, P.B., Tjoelker, M.G. and Bolstad, P.B., 2005. Foliar respiration acclimation to temperature and temperature variable Q_{10} alter ecosystem carbon balance. Global Change Biology, 11: 435-449.

Yavitt, J.B., Basiliko, N., Turetsky, M.R. and Hay, A.G., 2006. Methanogenesis and methanogen diversity in three peatland types of the discontinuous permafrost zone, boreal western continental Canada. Geomicrobiology Journal, 23: 641-651.

Zhu, R.B., Liu, Y.S., Sun, L.G. and Xu, H., 2007. Methane emissions from two tundra wetlands in eastern Antarctica. Atmospheric Environment, 41: 4711-4722.

Zhuang, Q., Melillo, J.M., Kicklighter, D.W., Prinn, R.G., McGuire, A.D., Steudler, P.A., Felzer, B.S. and Hu, S., 2004. Methane fluxes between terrestrial ecosystems and the atmosphere at northern high latitudes during the past

century: A retrospective analysis with a process-based biogeochemistry model. Global Biogeochemical Cycles, 18: doi: 10.1029/2004GB002239.

4 Appendices

4.1 Appendix 1 - Water jacketed chamber

Moss samples were placed within a water jacketed chamber in order to evaluate aerobic methane production by *Sphagnum* spp. mosses, when exposed to UVB light (Figure 4.1). The chamber was charged with air from a tank. Air was then cycled through the chamber and tubing by a pump. I monitored moss and air temperature with thermocouples, and PPFD was measured by a gallium-arsenide PPFD sensor connected to a data logger (Figure 4.1). UVB light was provided by a fluorescent bulb, applying direct light to the moss samples. Lastly, air within the chamber was mixed with a fan.

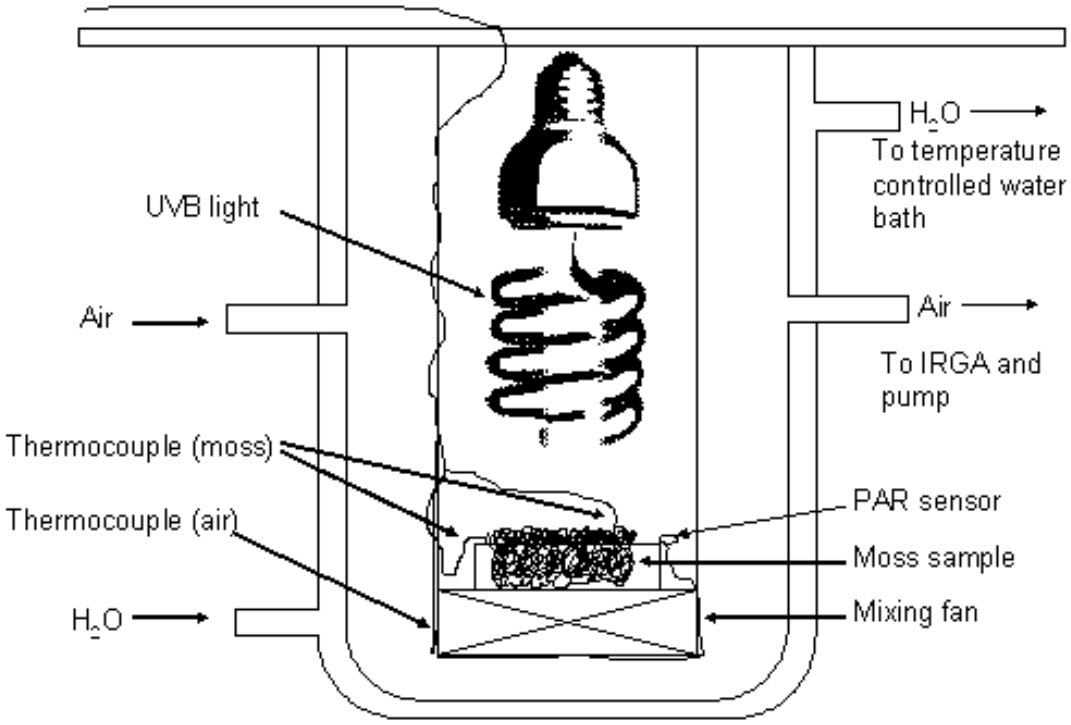

Figure 4.1. A schematic diagram of a water jacket chamber used to measure aerobic methane emission from *Sphagnum* spp. moss samples.

4.2 Appendix 2 - Closed chamber aerobic CH_4 flux measurement

I began aerobic methane production trials by first charging the chamber and tubing with tank gas. I allowed the chamber and tubing to charge until moss temperature equilibrated to our desired treatment temperature (Figure 4.2). Once the chamber was charged I then closed off the chamber and tubing to outside air, and cycled air through the system for 90 minutes (**Error! Reference source not found.**). After a 90 minute cycle, a 40 cc samples was drawn from a septum on tubing connected to the chamber. The 40 cc sample was then injected into a septum connected to the TGA100 in order to measure methane flux from moss samples.

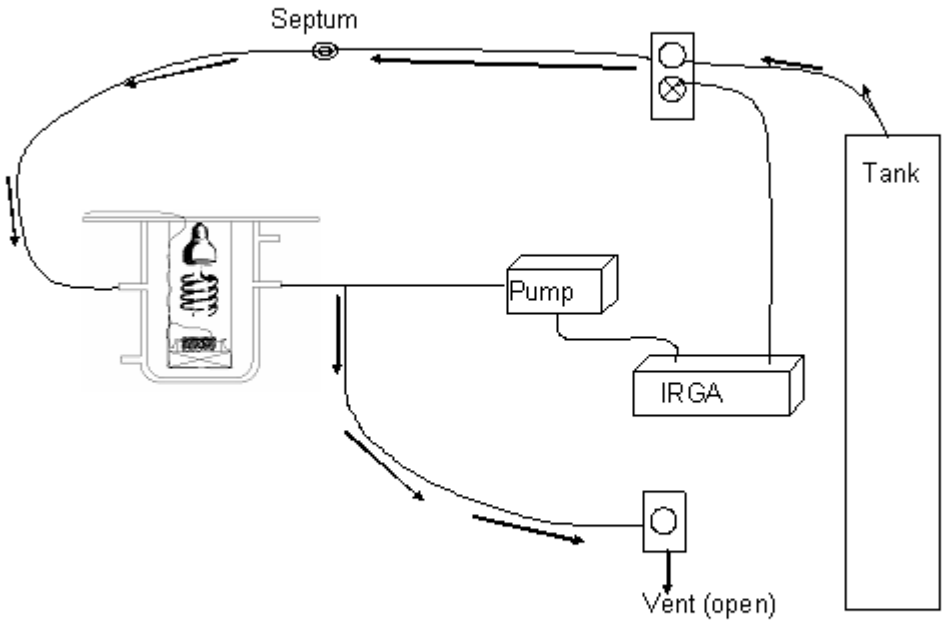

Figure 4.2. A schematic diagram of the chamber and tubing system charging with tank gas in order to conducted closed chamber measurements of aerobic methane production by *Sphagnum* spp. moss samples.

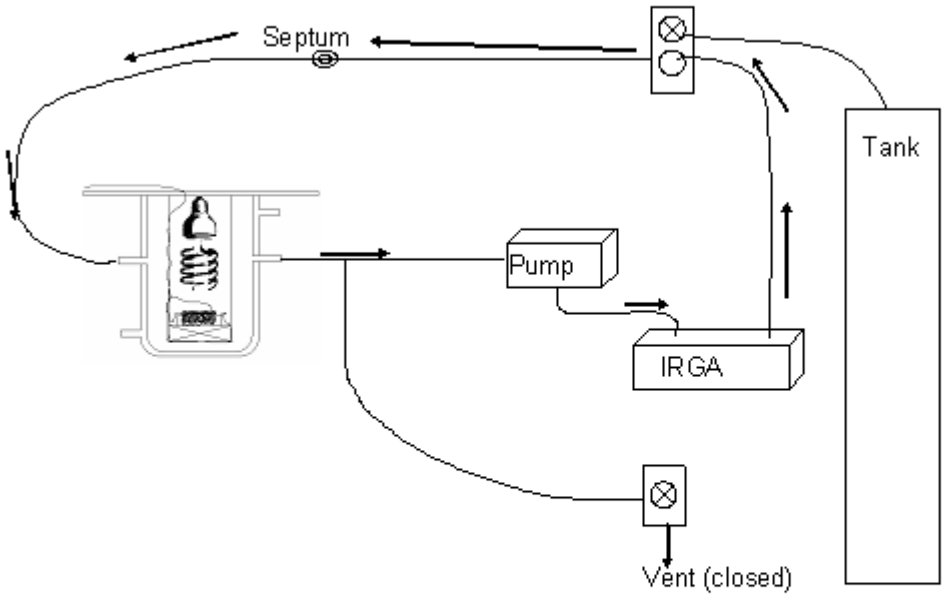

Figure 4.3. A schematic diagram of the chamber and tubing system with tank gas cycling throughout the tubing and chamber in order to conducted closed chamber measurements of aerobic methane production by *Sphagnum* spp. moss samples.